Institut des Nanotechnologies de Lyon UMR 5270

Métrologie des radiothérapies fractionnées spatialement et/ou à très hauts débits de dose : Détecteurs en microstrips scintillantes et détecteurs bimodaux

Patrick Pittet et al.

AG GDR Mi2B

Marseille, France, July 1, 2026

Introduction: trends in radiotherapy and dosimetry

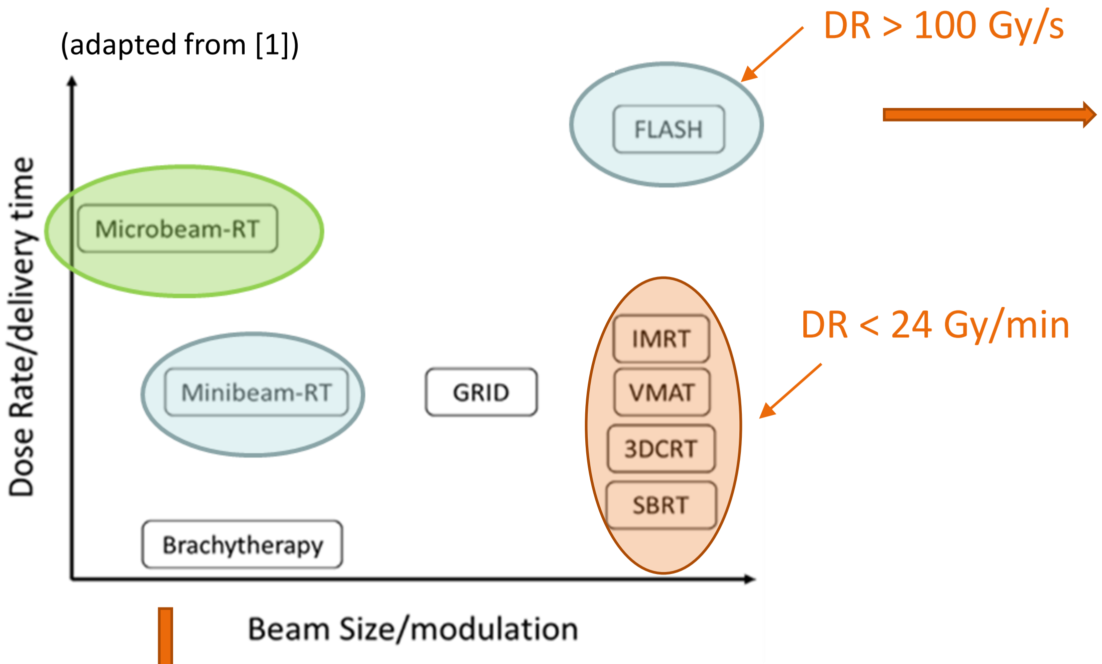

Radiation	Type	Source	Energy	Mean dose rate	Instantaneous dose rate
Protons	Medical	HyperScan	230MeV	200Gy/s	13kGy/s
X-rays	Synchrotron	ESRF / ANSTO	102keV	37Gy/s	18kGy/s
Electrons	Non-medical	Kinetron	4.5MeV	1000Gy/s	20MGy/s
Electrons	Medical	Clinac EX	9MeV	900Gy/s	1.7MGy/s
VHEE	Experimental	NLCTA	120MeV	90Gy/s	9×10^{12}Gy/s

(adapted from [2])

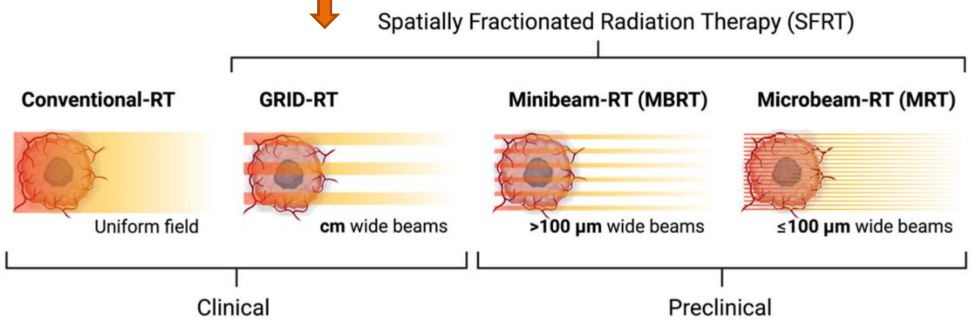

(adapted from [3])

[1] Griffin *et al.*, The British Journal of Radiology, vol. 93 (1113), 2020
[2] Esplen *et al* 2020 *Phys. Med. Biol.* **65** 23TR03)
[3] Fernandez-Palomo et al., *Cancers*, vol. 14(362), 2022

Introduction: trends in radiotherapy and dosimetry

☑ New treatment modalities bring with them new requirements for detectors, involving different technological choices

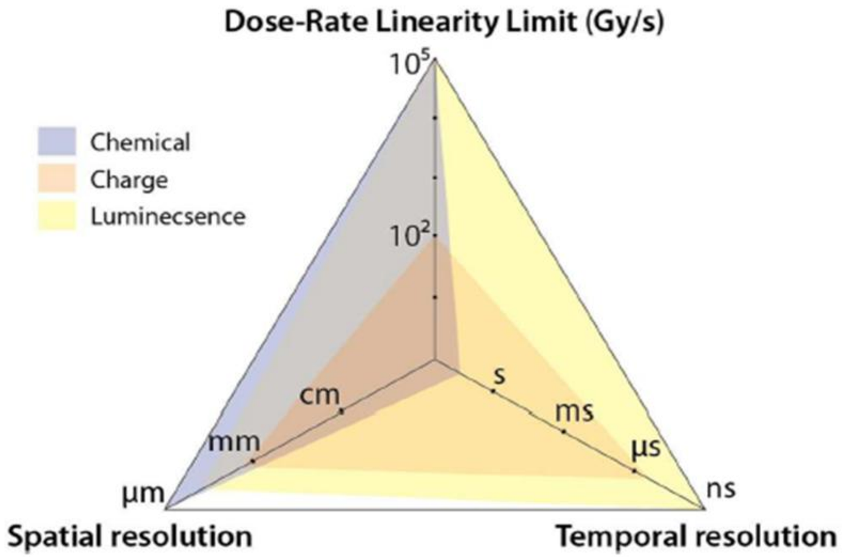

Adapted from [4]

→ Microstrip scintillating detectors

→ Bimodal Semiconductor detector

Institut des Nanotechnologies de Lyon UMR 5270

[4] Ashraf et al., *Front. Phys.* 8(328), 2020

Introduction: scintillating microstrips vs fibers for MRT

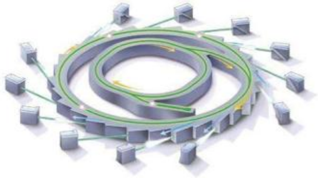

X-ray synchrotron source
Energy: 50 – 250 keV

Wide X-ray Dose rate range
@Peak: 10^2-10^4 Gy/s

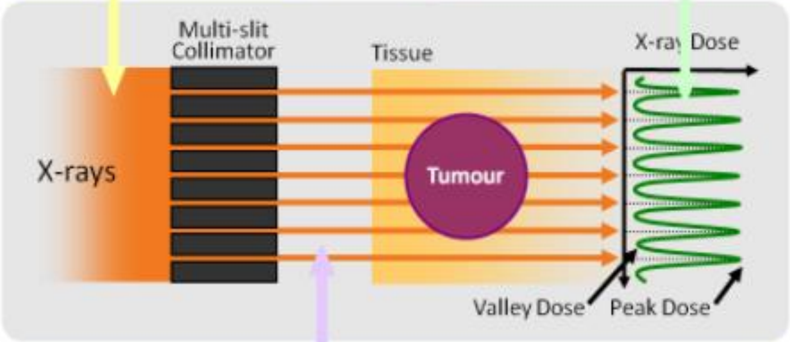

An array of micro-structured X-ray beams
HWFM: 20-100 µm pitch: 100–413 µm

Adapted from [5]

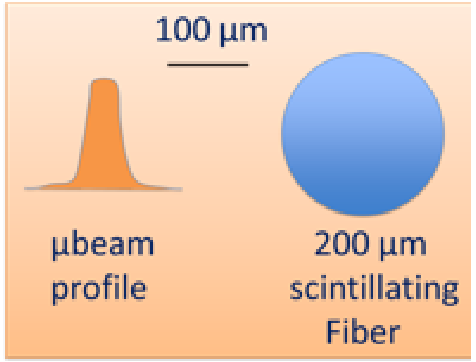

Institut des Nanotechnologies de Lyon UMR 5270

[5] Koziol et al. University of Science and Technology AGH, Krakow, Poland 08.03.2016

Introduction: scintillating microstrips vs fibers for MRT

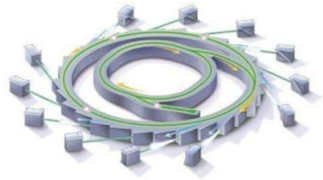

X-ray synchrotron source
Energy: 50 – 250 keV

Wide X-ray Dose rate range
@Peak: 10^2-10^4 Gy/s

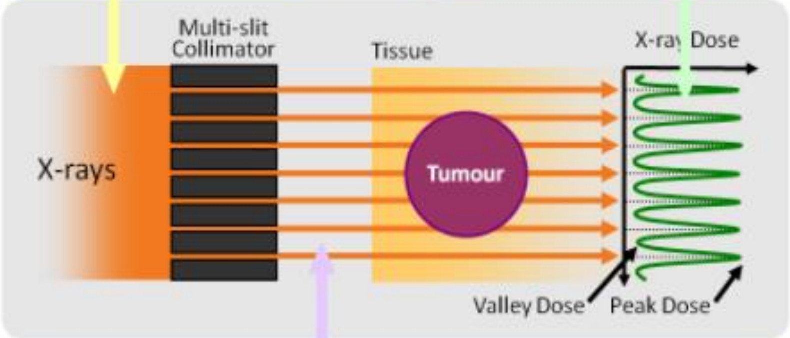

An array of micro-structured X-ray beams
HWFM: 20-100 µm pitch: 100–413 µm

Adapted from [5]

Planar technology
for scintillating strip microfabrication

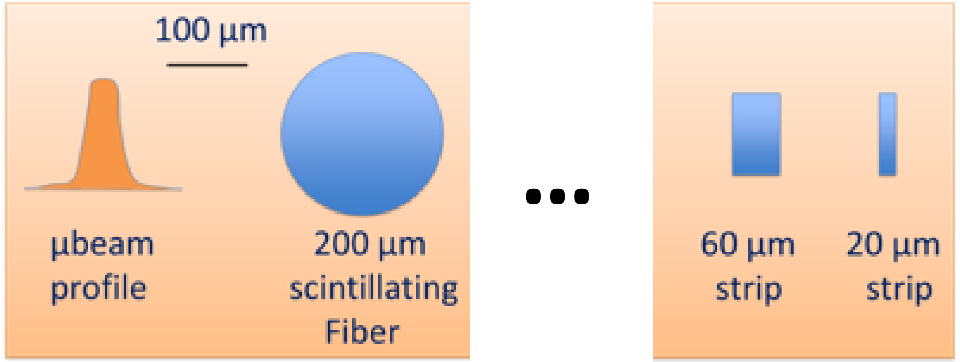

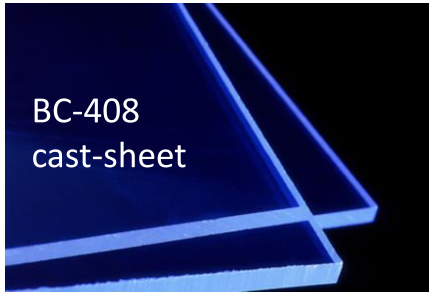

based on a
long-established material

based on QDots

[5] Koziol et al. University of Science and Technology AGH, Krakow, Poland 08.03.2016

BC-408 based microstrip scintillating detector system

PhD Florian Thevenet

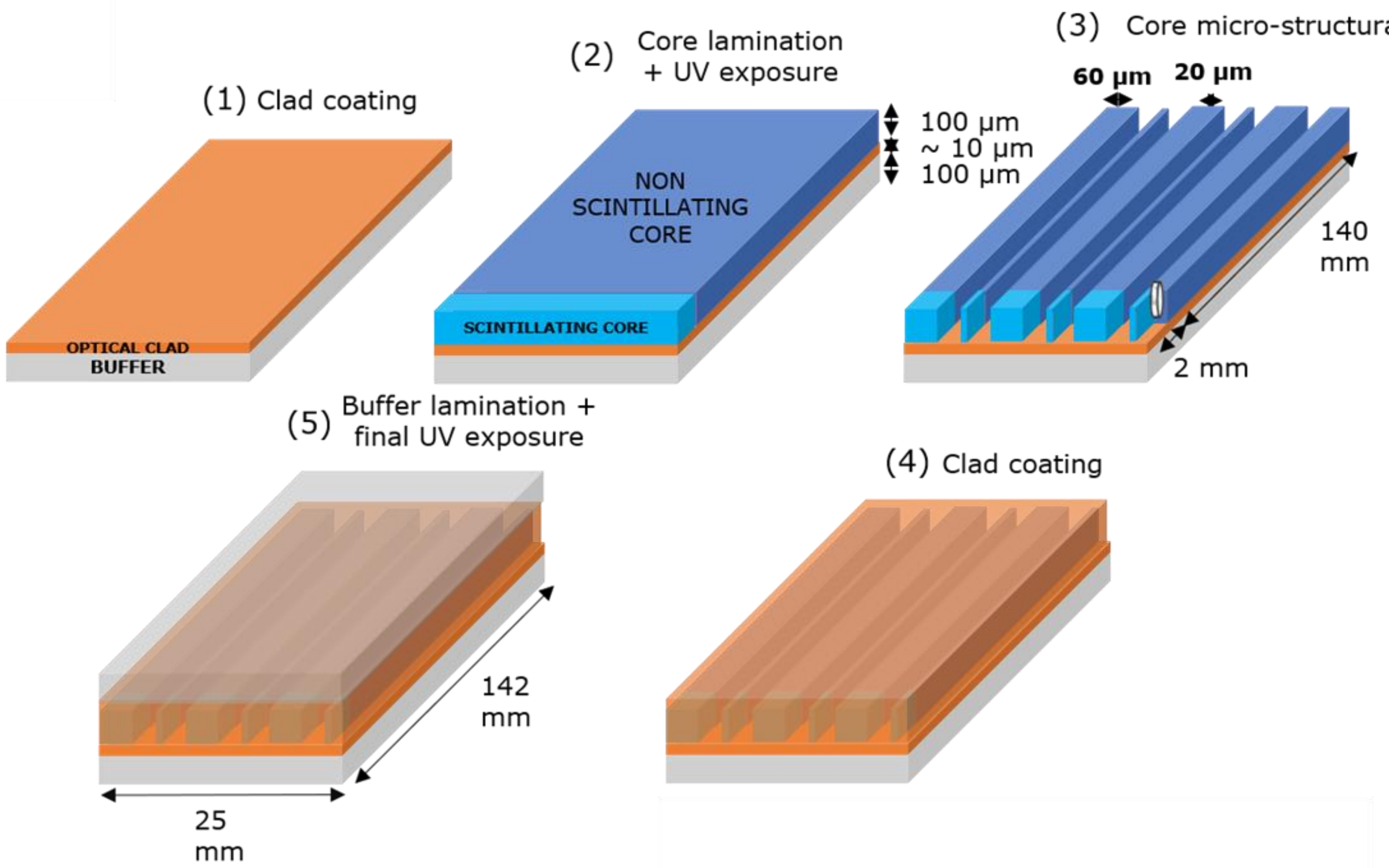

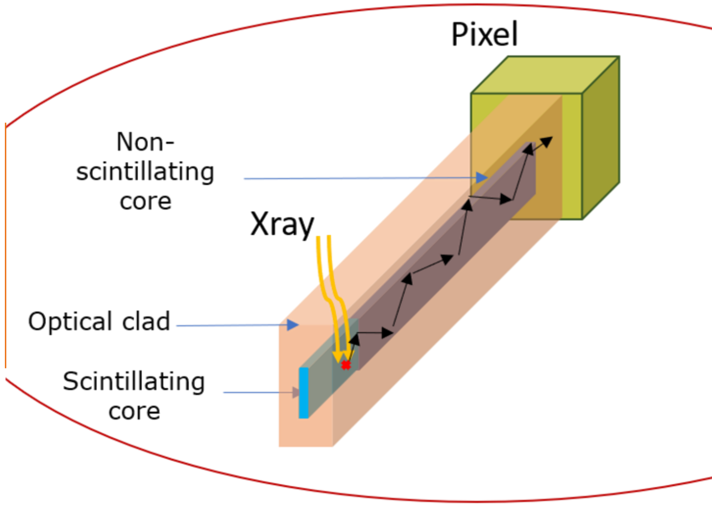

- ✓ implementation of a high number of microstrips for the full MRT field monitoring (>100 channels)
- ✓ self-alignment of scintillating and clear strips

Institut des Nanotechnologies de Lyon UMR 5270

BC-408 based microstrip scintillating detector system

PhD Florian Thevenet

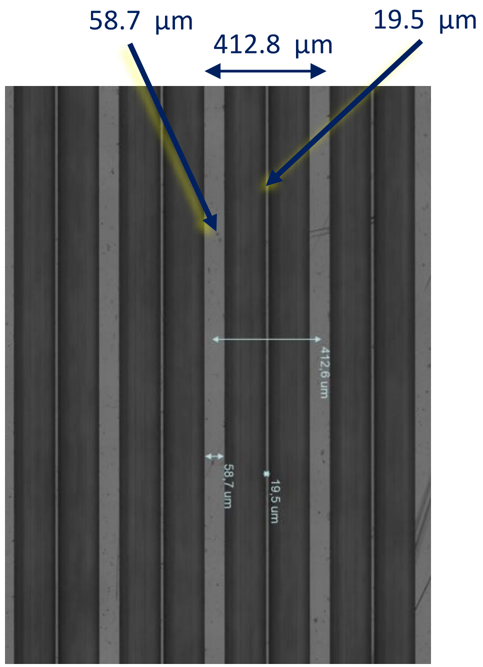

Image of µ-microstructure BC408 layer

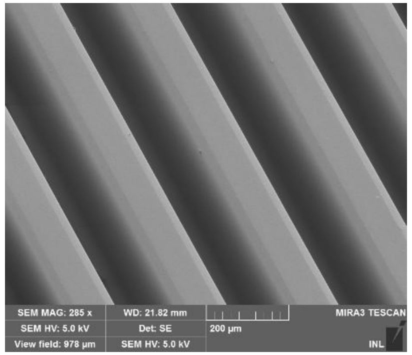

Scanning electron microscope image of micro-structured cores

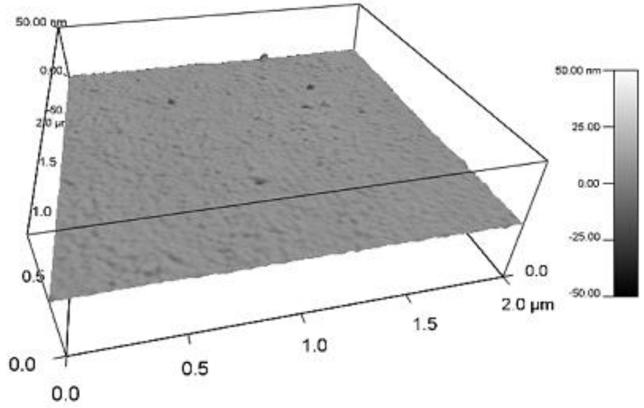

Optical grade surface roughness measured by Atomic Force Microscopy
($\sigma_{rms} = 7nm\ over\ 20x20\mu m^2$)

Institut des Nanotechnologies de Lyon UMR 5270

BC-408 based microstrip scintillating detector system

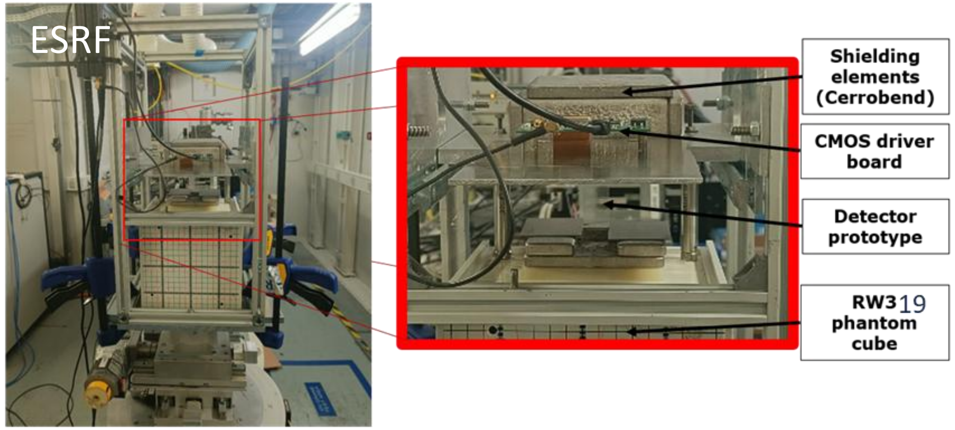

5.4 kGy/s

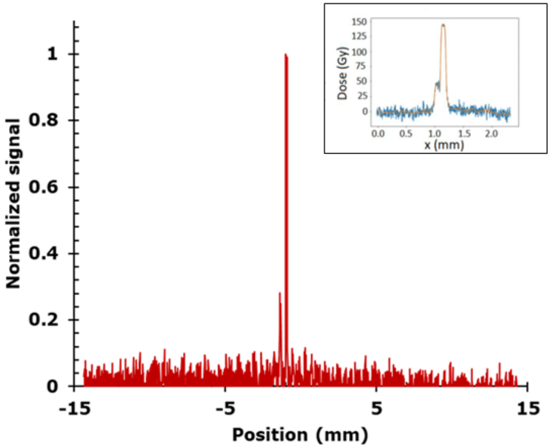

PhD Florian Thevenet

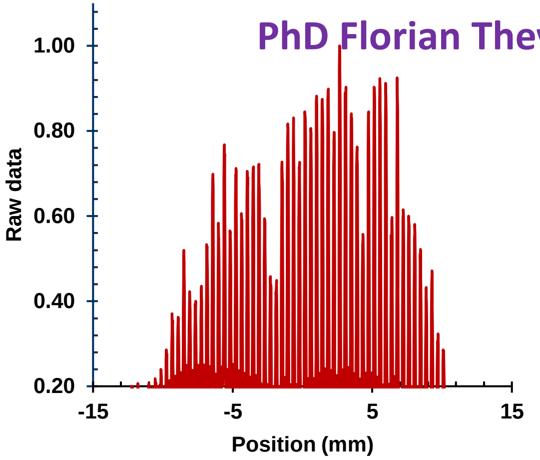

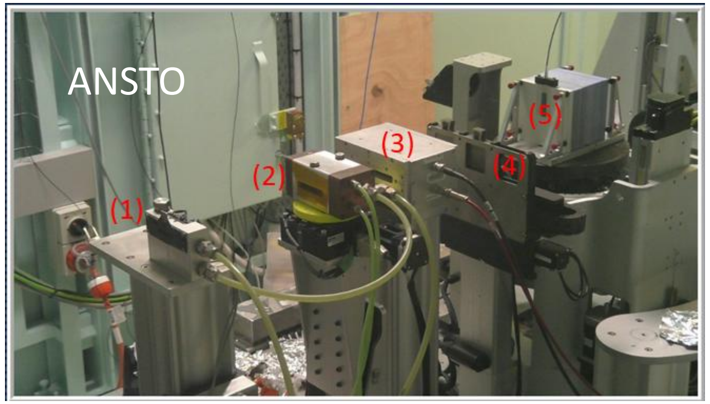

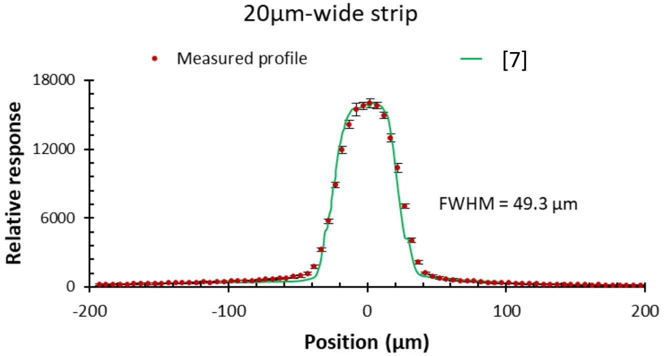

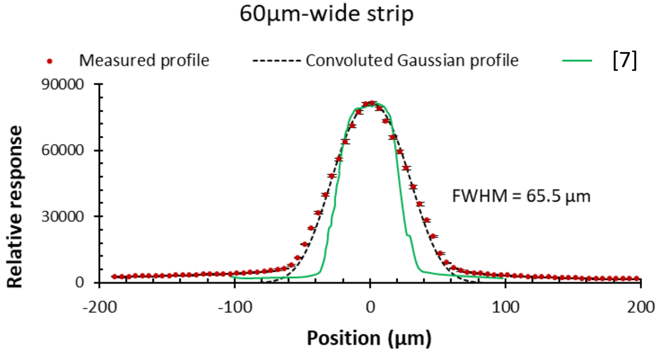

(1) Beam-Defining Aperture (BDA)
(2) Multislit collimator
(3) Ionization chamber
(4) Mask assembly
(5) RW3 slab phantom with detector at 2 cm depth using clear fibers instead of clear strips

163 Gy/s
Mean Beam energy: 95 keV

20µm-wide strip PVDR (S_{CuCu})

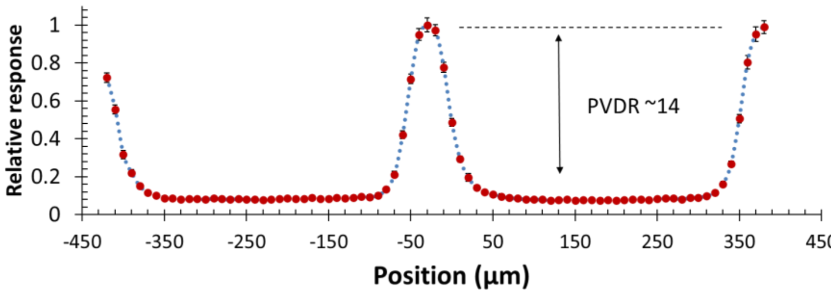

Institut des Nanotechnologies de Lyon UMR 5270

[6] F. Thevenet et al., Sci. Reports vol. 15(1), 2025
[7] J. Livingstone et al., Med. Phys., vol. 43(7), 2016

Double-clad QDot-based microstrip detector for SFRT

In this study, we developed QDot-based microstrip detector implementing heterogeneous active volume[12] with:

- CdSe QDots as nano-scintillators[13]
- Organic tissue-equivalent surrounding material (Photoresist and Cyclic Olefin Copolymer COC)

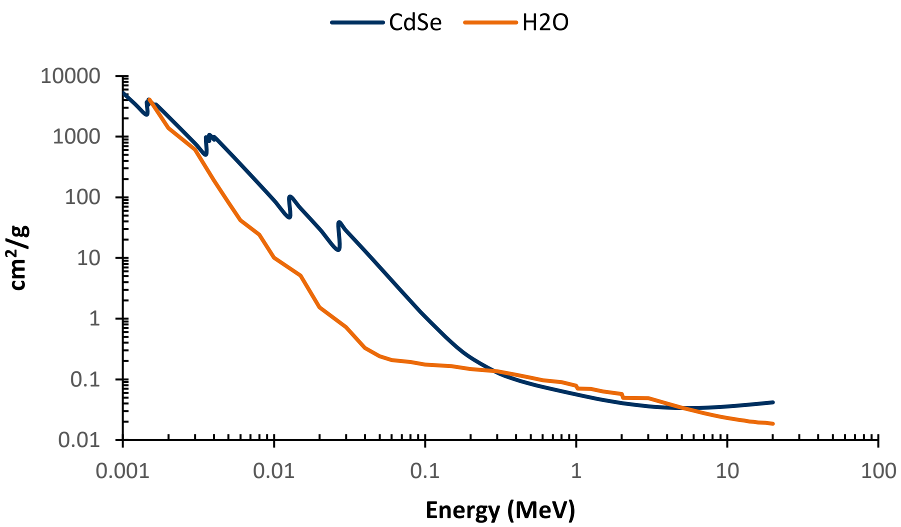

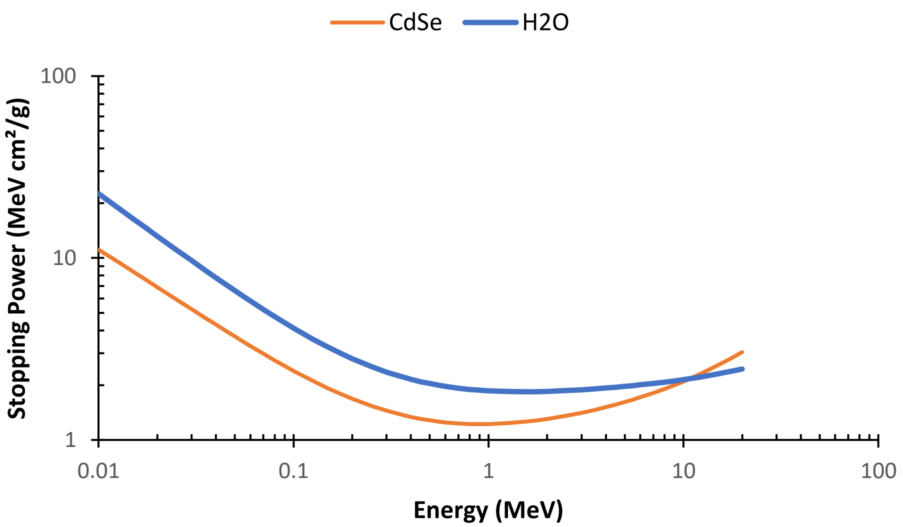

For lower energy dependence of the strips, the scintillators should verify the Bragg-Gray conditions (small cavity)

Institut des Nanotechnologies de Lyon UMR 5270

[12] *F. Thevenet et al., J. Phys.: Conf. Ser. 2799 012012, 2024*
[13] C. Dujardin et al., *Adv. Optical Mater.*, 13, 2402739, 2025

Double-clad QDot-based microstrip detector for SFRT

BG C1 : QDot size (< 100 nm) is much smaller than the range of charged particles

☞ no perturbation of the fluence of charged particles in the medium

ESTAR - NIST

Electron range

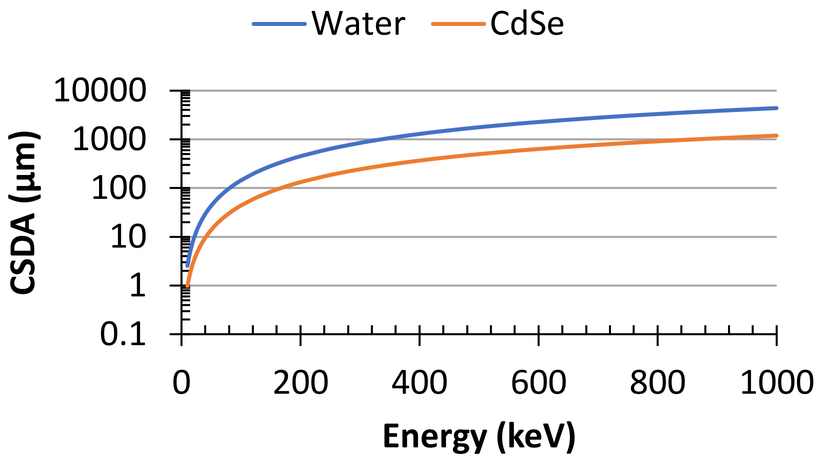

BG C2 : The energy absorbed in the QDot comes exclusively from charged particles passing through the cavity

☞ very low QDot concentration

Each Qdot can be considered as a Bragg-Gray "cavity"

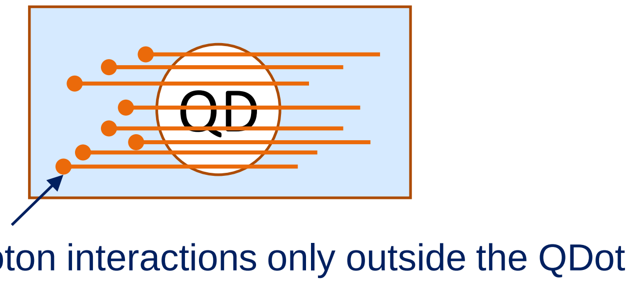

Institut des Nanotechnologies de Lyon UMR 5270

Double-clad QDot-based microstrip

Refractive index management for implementation of multimode double-clad waveguides

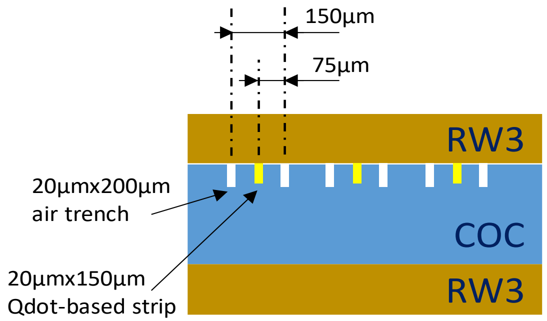

Refractive index of the photoresist ~1.60 (core)

Refractive index of cyclo-olefin copolymer (COC) ~ 1.53 (1^{st} clad)

Refractive index of air = 1 (2^{nd} clad)

https://phydemo.app/rayoptics/simulator/

QDot Loaded photoresist
(scintillating microstrip)

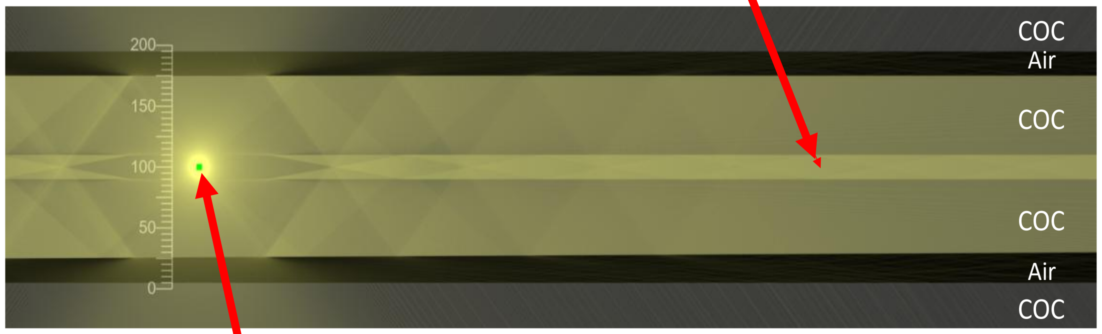

QDot
luminescence

Institut des Nanotechnologies de Lyon UMR 5270

Results: SEM and EDS microstrip characterization

Elemental composition of the strip

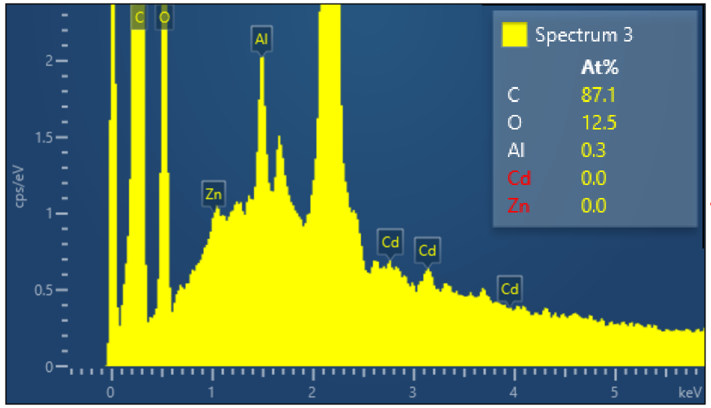

SEM Image

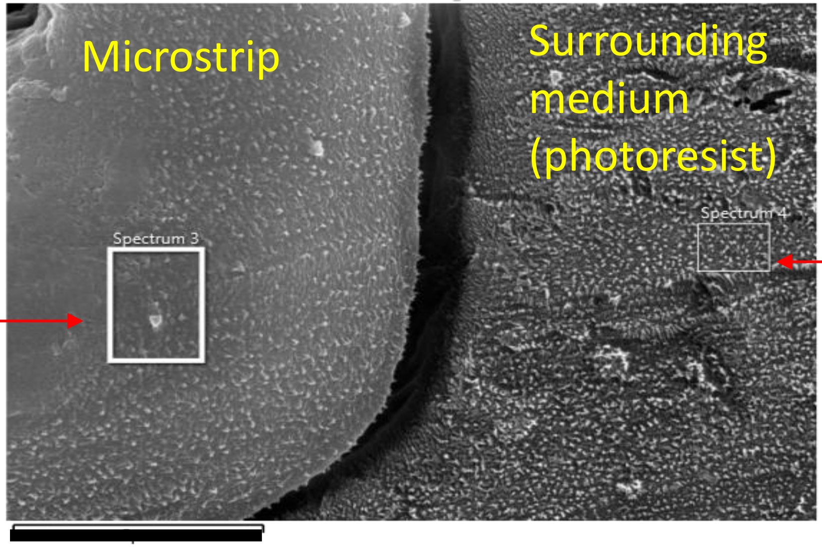

5 µm

Elemental composition of the surrounding medium (photoresist)

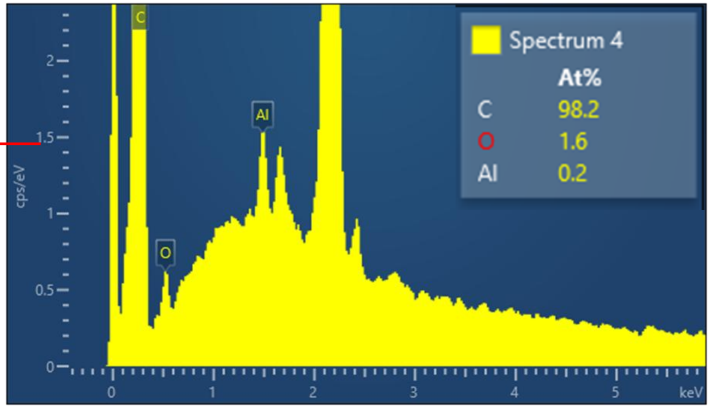

☞ Scanning electron microscopy with energy-dispersive X-ray spectroscopy (SEM/EDS) confirms low CdSe QD concentration in the strip, wit

limited particle aggregations

Results: UV-microscope images of the detector

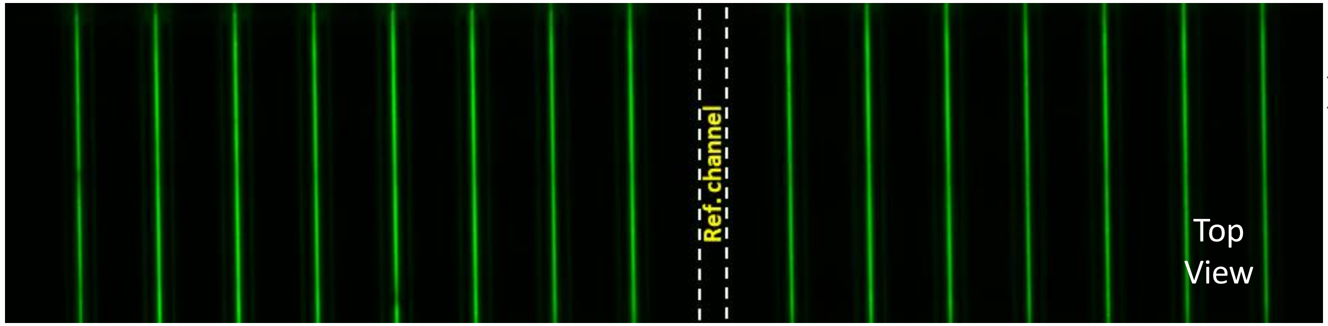

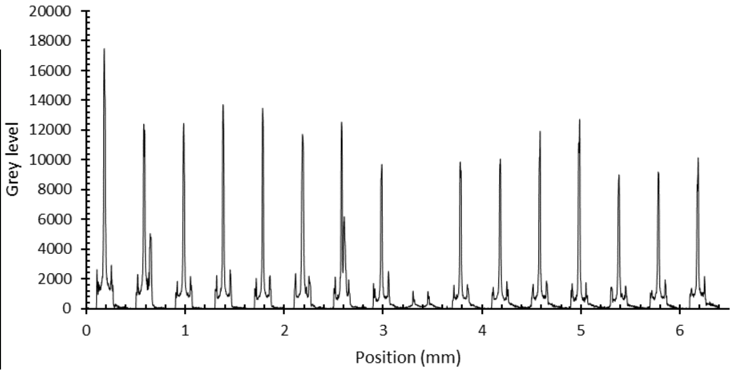

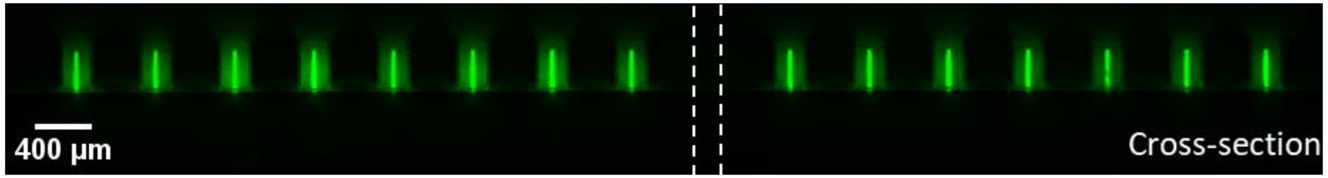

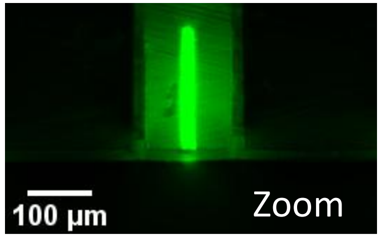

- ✓ Bright UV-Fluorescence of each microstrip
  - ☞ good dispersion and passivation of the CdSe Qdots
  - ☞ the waveguide core shows the 20 µm x 150 µm microstrip cross-section
- ✓ The double-clads guide the fluorescence

Institut des Nanotechnologies de Lyon UMR 5270

Material and Methods: Characterization setups

- Synchrotron characterization:

  - ESRF (BM05): 40keV monochromatic X-ray microbeam with 10^{10}ph/s in 2x2mm² radiation field upstream the focusing lens

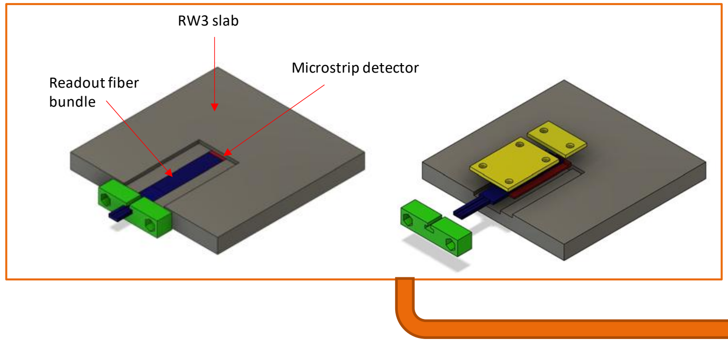

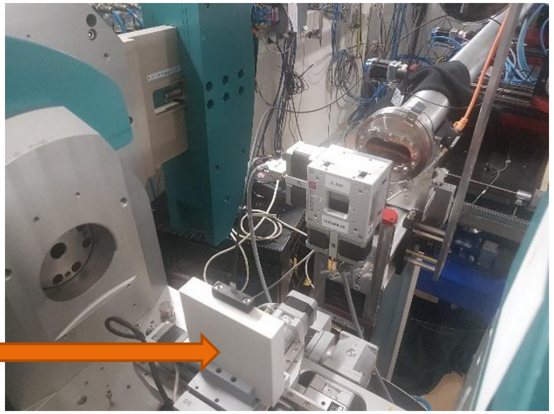

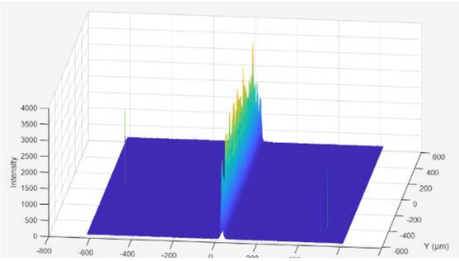

Microbeam profile (40 keV)

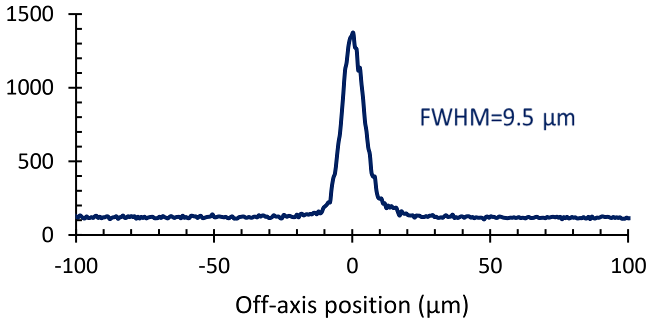

  - ANSTO (IMBL): Mean beam energy 52 keV to 123 keV – Dose rate up to 4750 G/s

Institut des Nanotechnologies de Lyon UMR 5270

Results: ESRF measurements

UV fluorescence image

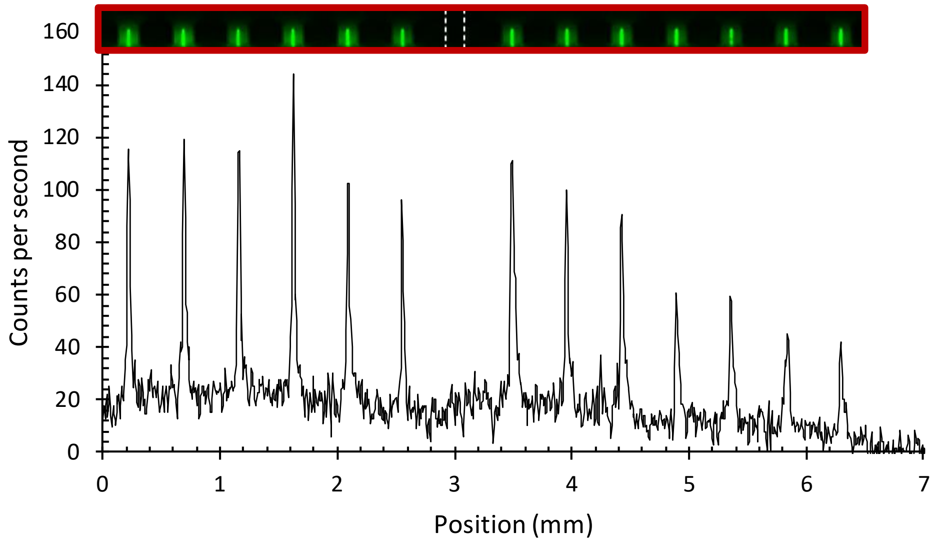

X-ray µbeam scan (20 µm steps)

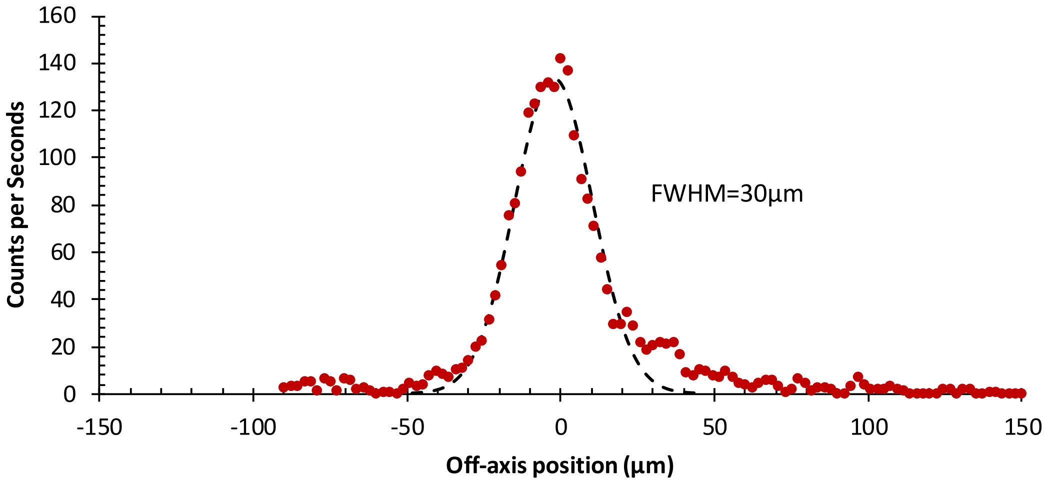

X-ray µbeam scan (2.5 µm steps)

✓ Detectable luminescence for each microstrip

Results: ESRF measurements

UV fluorescence image

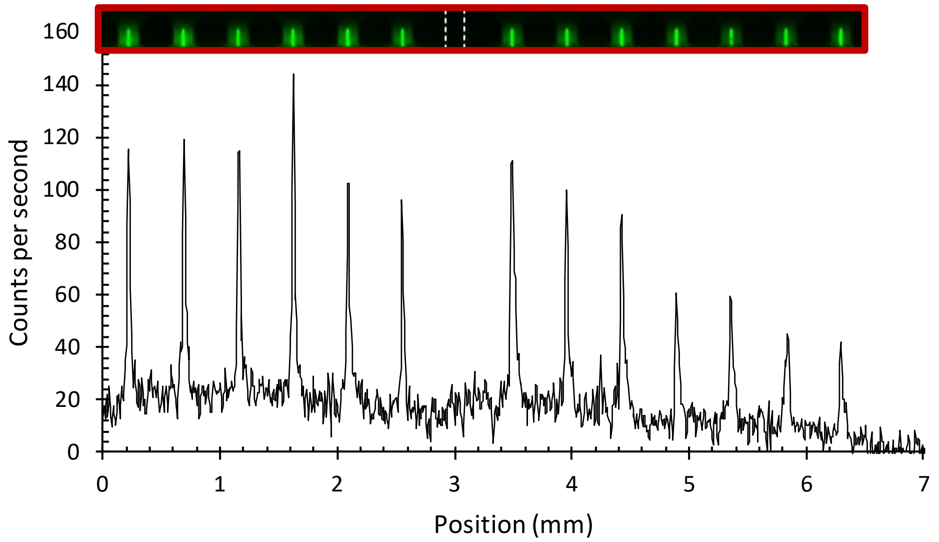

X-ray µbeam scan (20 µm steps)

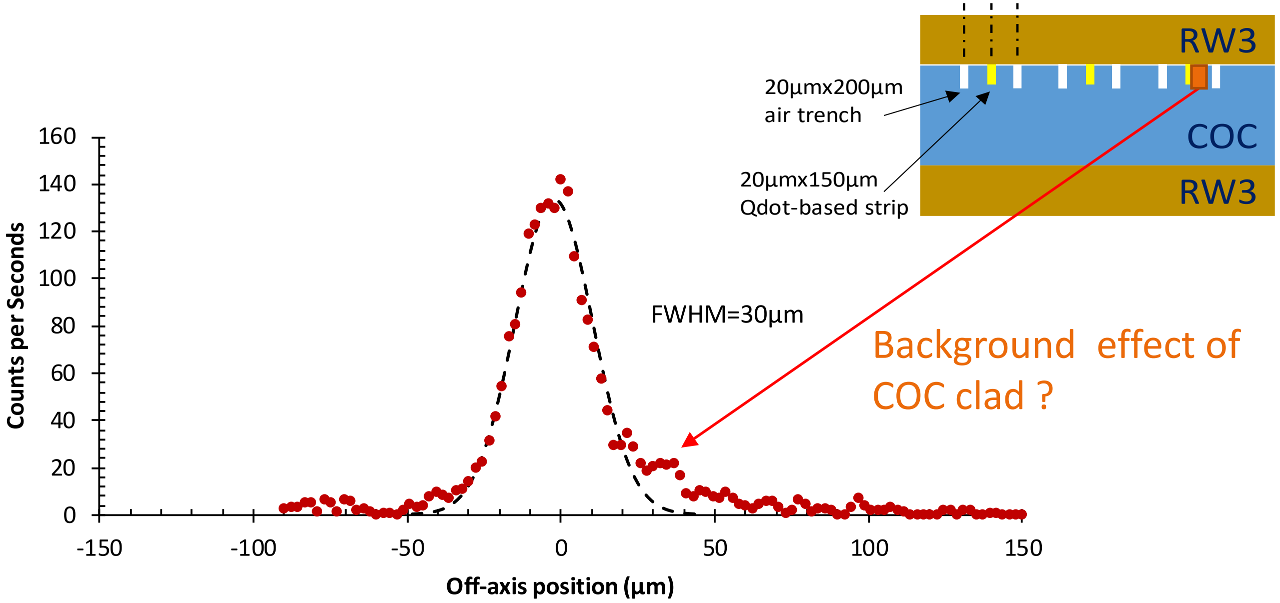

X-ray µbeam scan (2.5 µm steps)

Microbeam profile (40 keV)

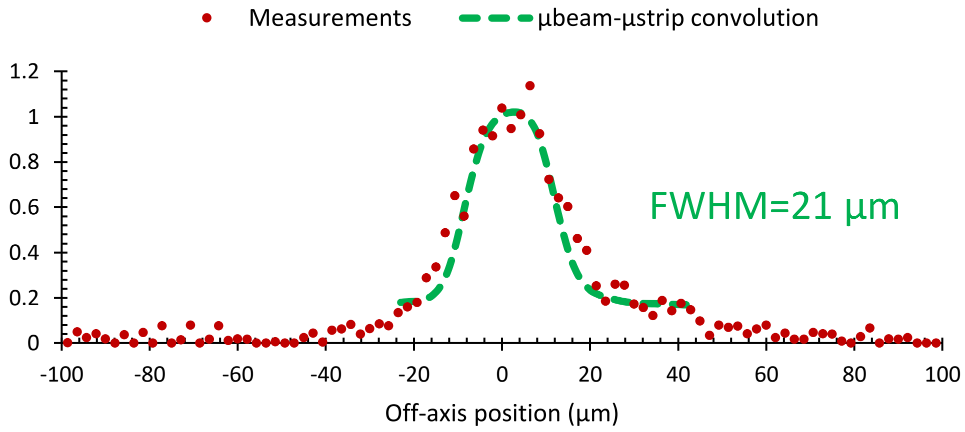

- ✓ Detectable luminescence for each microstrip
- ✓ Peak broadening (volume averaging effect) with COC Clad stem effect

Institut des Nanotechnologies de Lyon UMR 5270

Results: ANSTO IMBL measurements

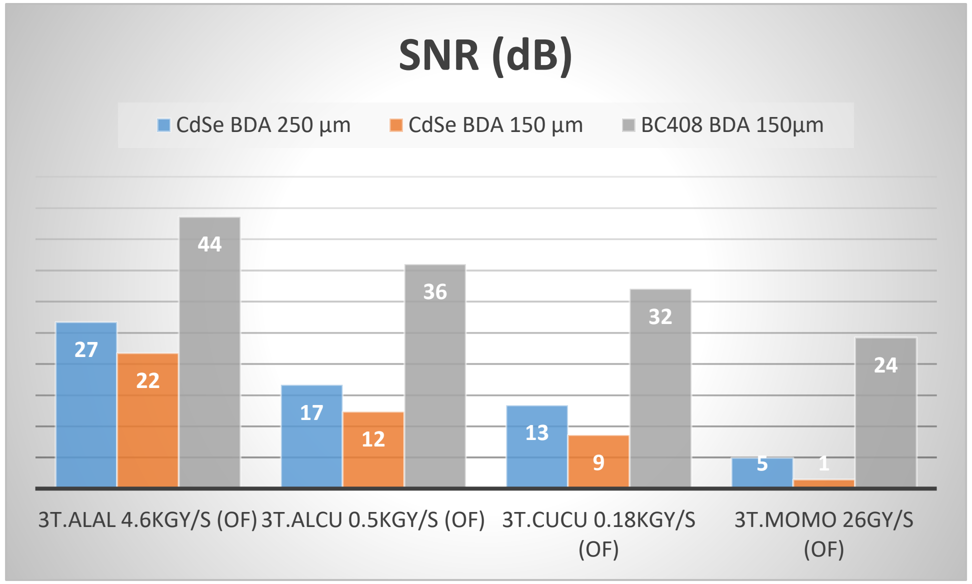

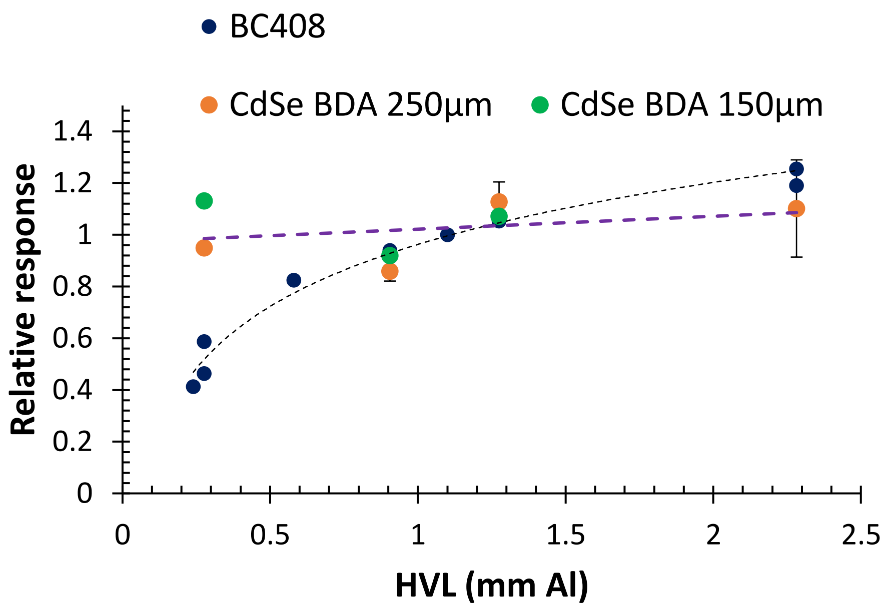

- ✓ SNR was much lower than with BC408 strips (-20 dB)
- ✓ Energy dependence seems to be much lower than with BC408 (to be confirmed)

Institut des Nanotechnologies de Lyon UMR 5270

Discussion

- BC-408-based have been fabricated and tested
  - ☞ 20 µm microstrips provide suitable spatial resolution for µbeam QA in MRT
  - ☞ We observed a yield drop between 60 µm and 20 µm wide strips (Two dopant scintillation mechanism)

- Double-Clad Qdot-based microstrips have been fabricated and tested
  - ☞Ligand engineering allows good dispersity of QDots in photoresist
  - ☞Luminescence guidance has been confirmed by UV-fluorescence measurements
  - ☞ under X-ray irradiation, a background con,tribution was attributed to the width of the 2nd Clad
- CdSe quantum dot microstrips have produced measurable signals
  - ☞encouraging preliminary results during irradiation with high dose rate µbeam (remained to be confirmed)
  - ☞SNR was 20 dB lower than with BC-408 microstrips
  - ☞ Qdot concentration should be optimized for SNR increase while maintaining strip density ~1, low self-absorption and aggregation
- All tests where carried out with static fields while MRT implements dynamic fields
  - ☞ Stem effect issues need to be addressed (2nd Clad + Readout clear fiber bundle)

Institut des Nanotechnologies de Lyon UMR 5270

Bimodal Ga_2O_3-based X-ray detectors for FLASH therapies

X-ray detection in Ga2O3

X-ray absorbed dose in semiconductors [14]

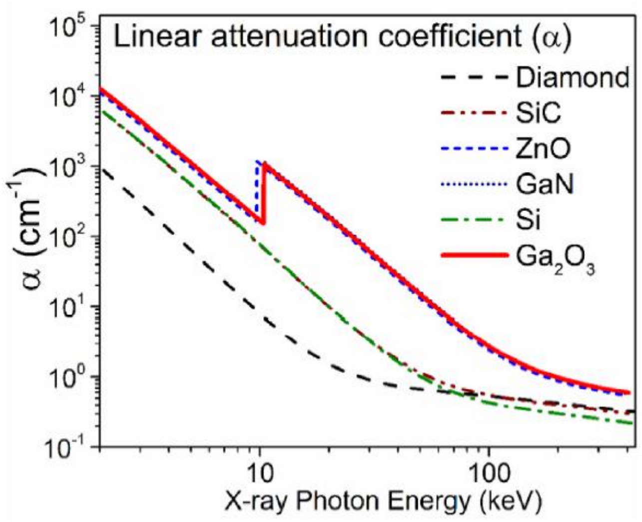

Electron–hole pair creation energy in semiconductors

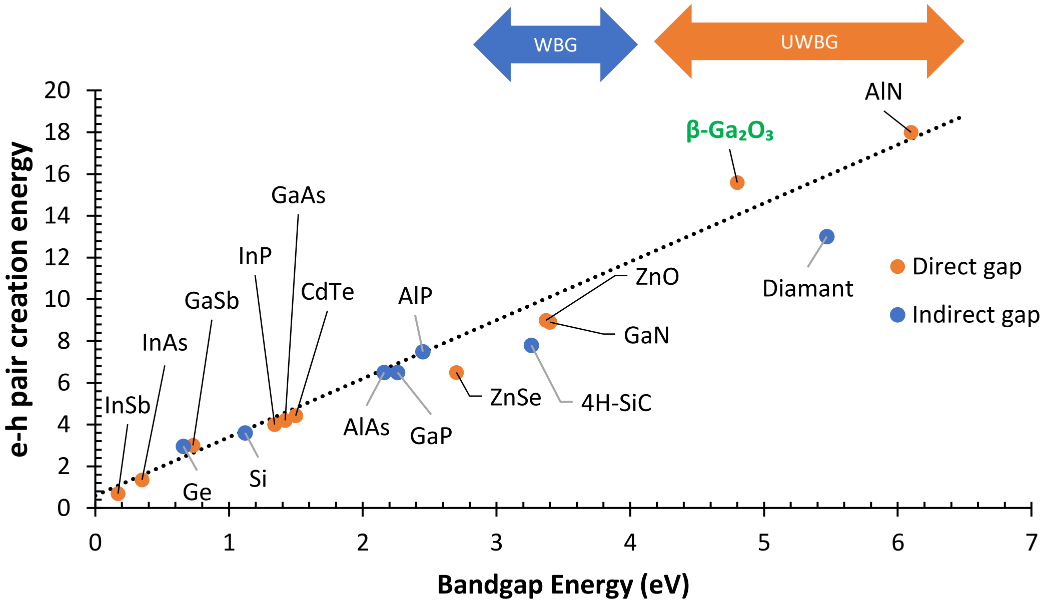

- Direct-gap semiconductors $\rightarrow$ High probability of radiative e-h pair recombination
- WBG and UWBG $\rightarrow$ lower dark-current, higher breakdown fields, superior radiation tolerance [15]

[14] https://doi.org/10.1016/j.mtphys.2023.101095
[15] https://doi.org/10.1088/1361-6528/adb8f2

X-ray detection in Ga2O3

Luminescence

Charge

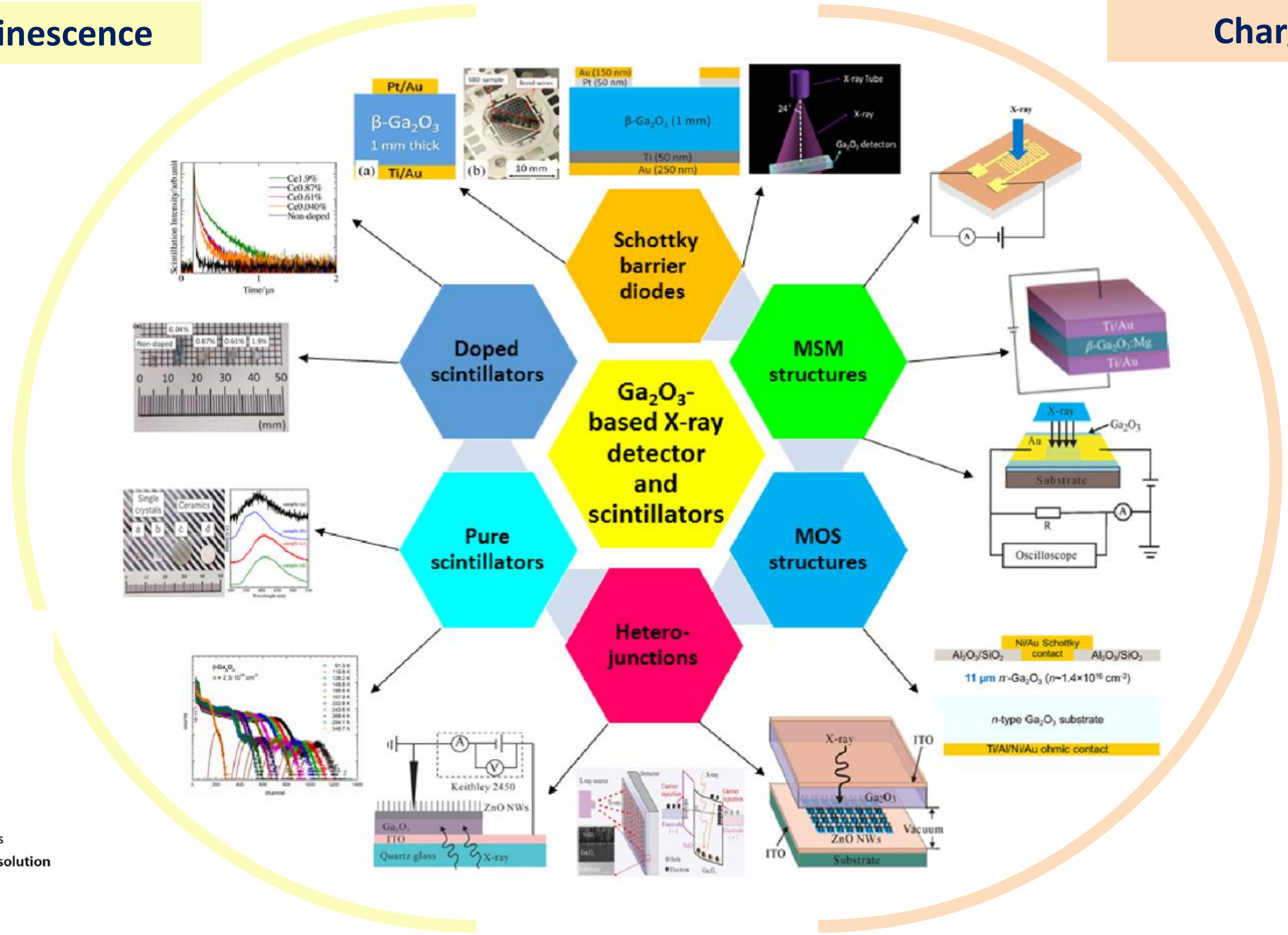

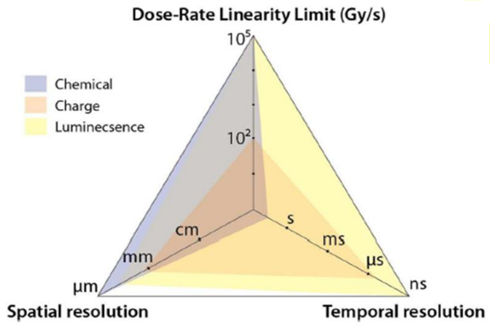

[16] https://doi.org/10.1016/j.mtphys.2023.101095

Institut des Nanotechnologies de Lyon UMR 5270

X-ray detection in Ga2O3

Luminescence

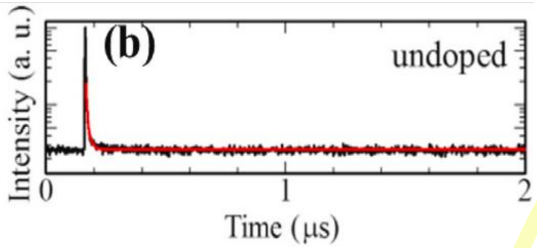

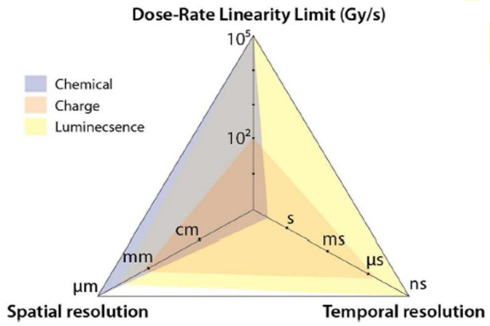

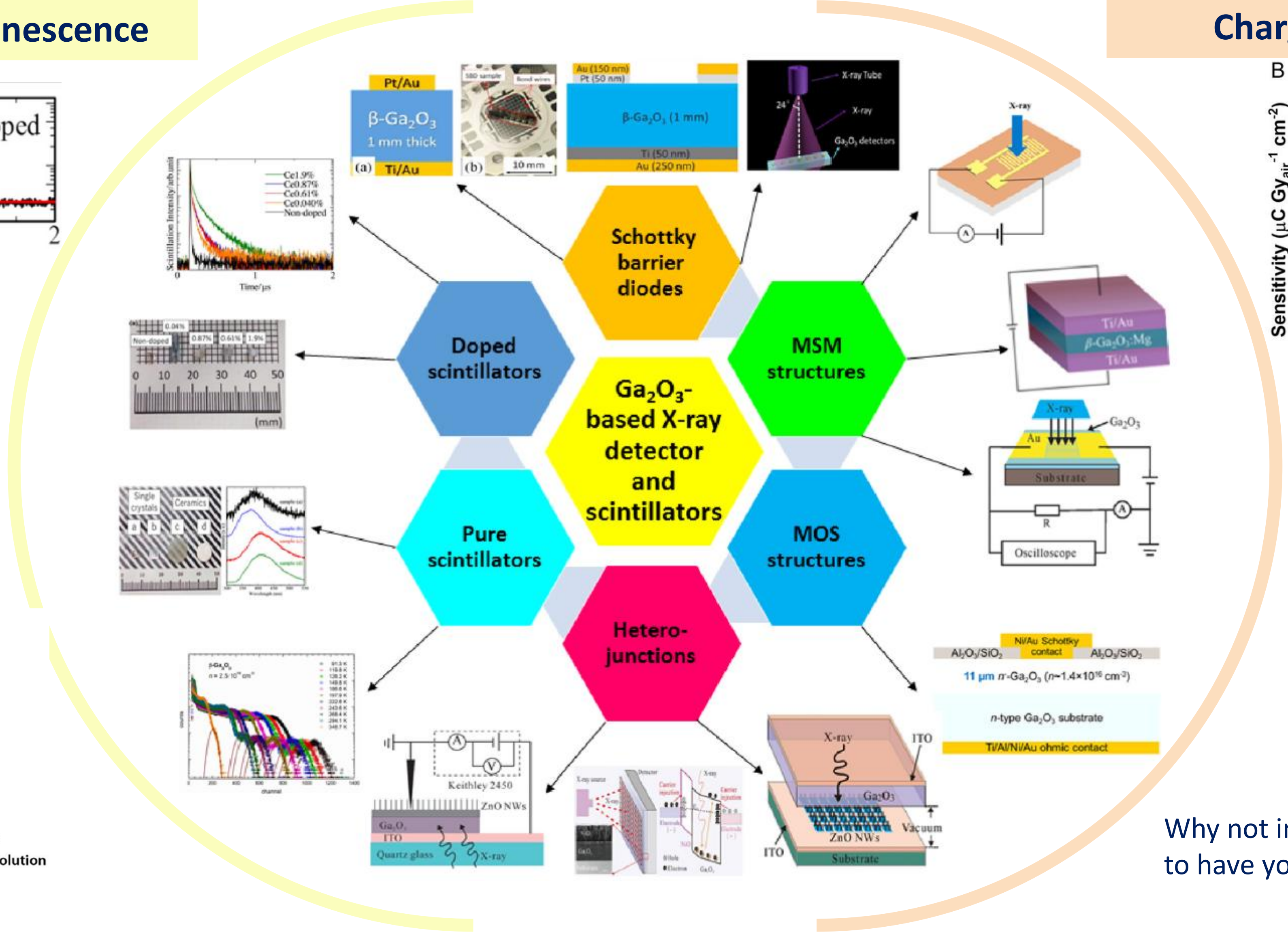

Charge

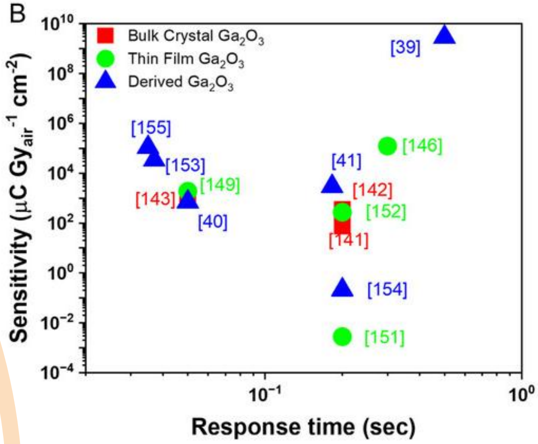

Why not implement bimodal transduction to have your cake and eat it too?

Institut des Nanotechnologies de Lyon UMR 5270

[16] https://doi.org/10.1016/j.mtphys.2023.101095
[17] https://doi.org/10.1088/1361-6463/ad8e6e

Ga2O3 MSM detector prototypes

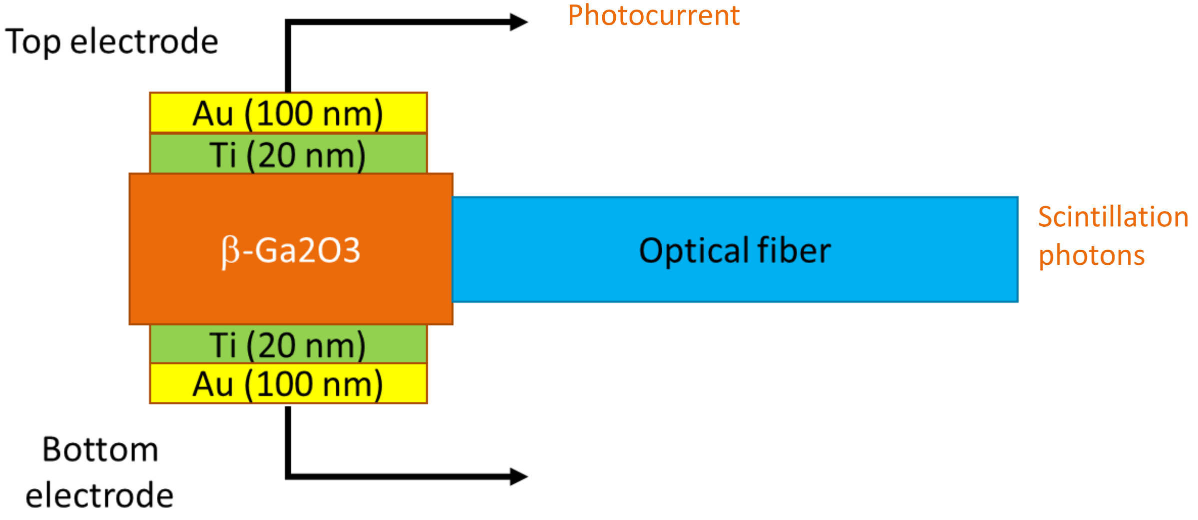

X-ray image of one prototype

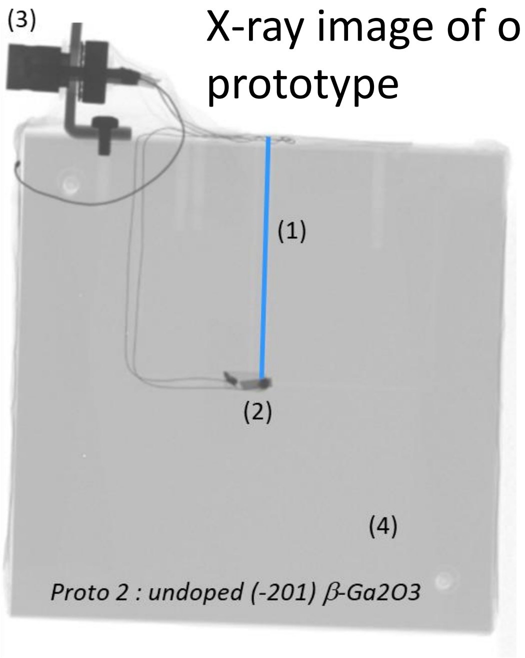

(1) Fiber channel
(2) Ga2O3 substrate
(3) BNC connector
(4) 10x10 cm² RW3 tissue-equivalent slab

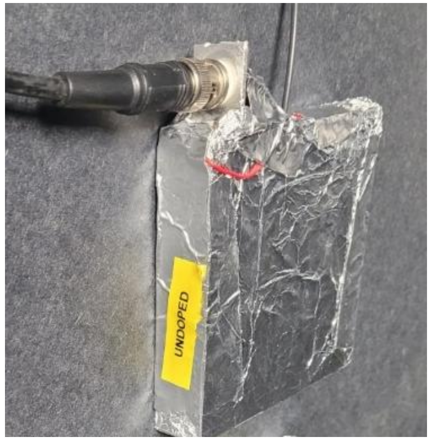

Bimodal readout module

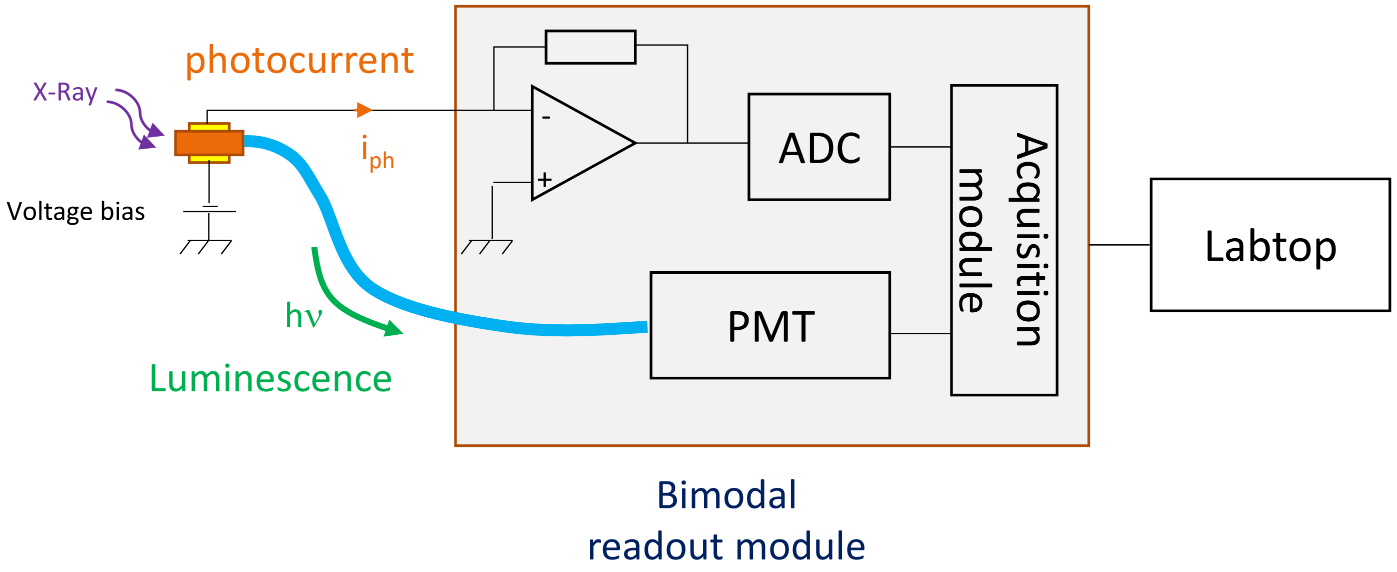

Irradiation setup at the ANSTO IMBL

Dosimetric response of Ga2O3

e-h creation energy	Photogenerated pair density	For a single µbeam (FWHM=50µm BDA=150µm)	For a single µbeam (FWHM=50µm BDA=150µm) @ flash Dose rates
15.6 eV [9]	~2.6 10^{13} e-h pair/cm^3/Gy$_{Ga2O3}$	~10^8 e-h pair/Gy$_{Ga2O3}$	more than 10^{10} e-h pair/s

X-ray spectra at Australian synchrotron

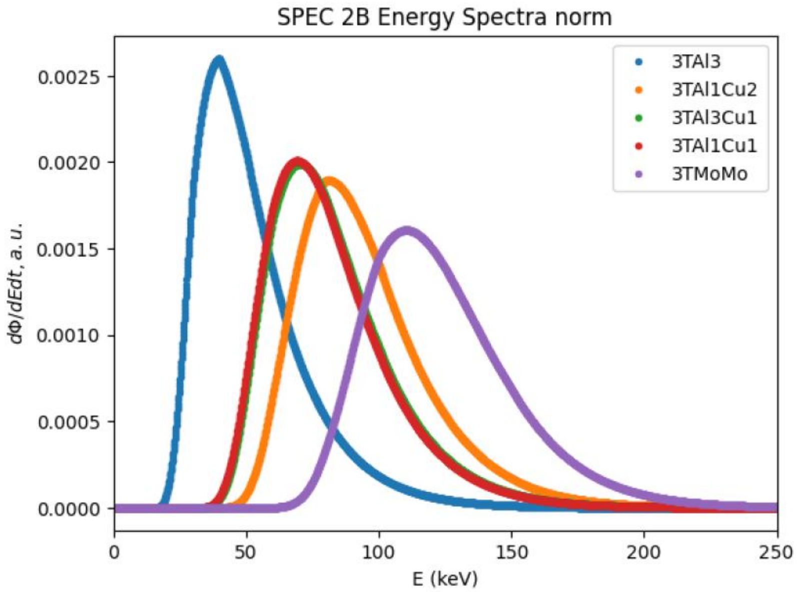

[9] https://doi.org/10.1063/5.0053301

Institut des Nanotechnologies de Lyon UMR 5270

self-absorption of the scintillation signal (IMBL – ANSTO)

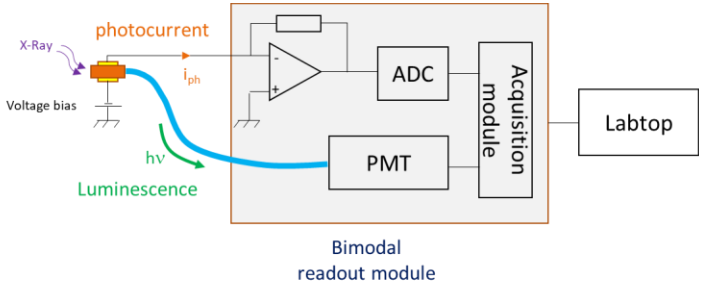

Dose rate: 4749 Gy/s
Mean beam energy: 52.32 keV
Continuous translation of the microbeam

UID prototype

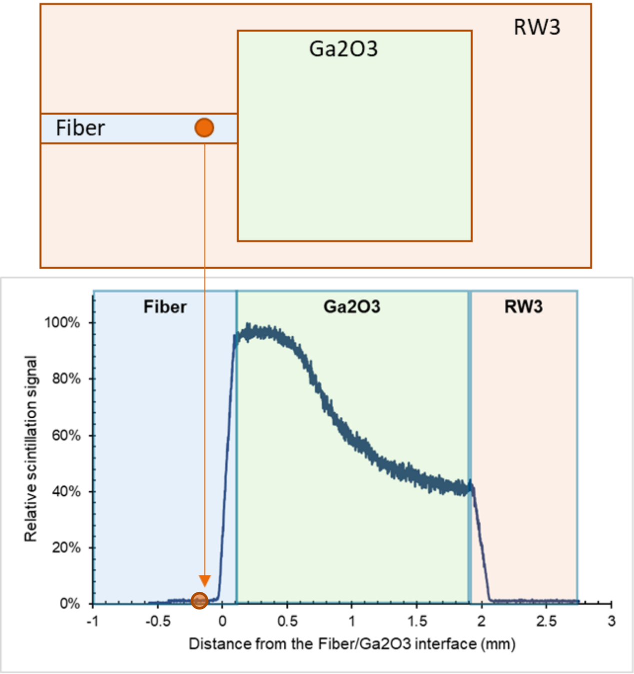

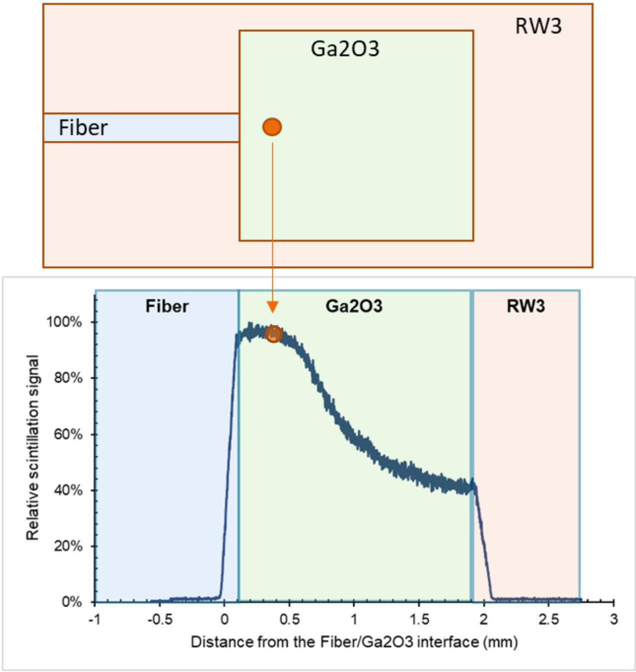

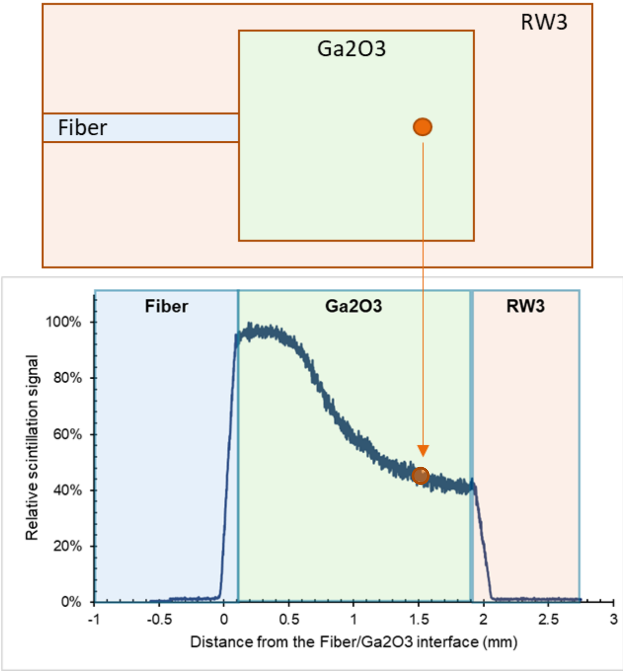

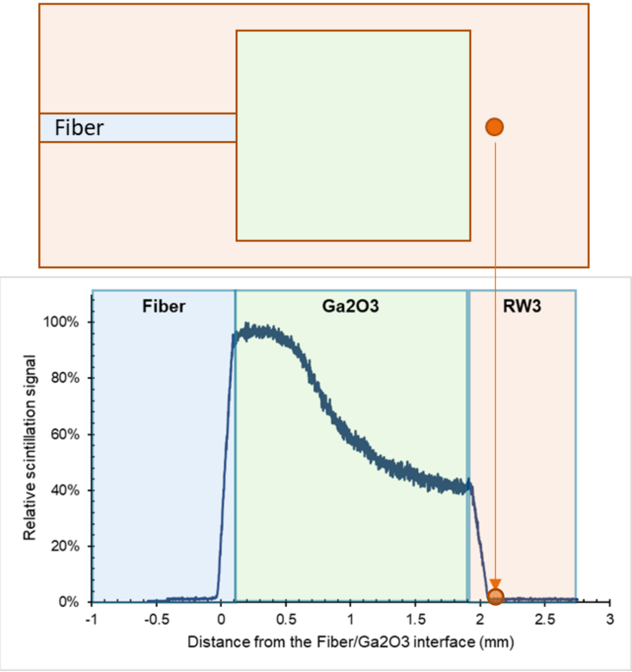

Institut des Nanotechnologies de Lyon UMR 5270

Radiation tolerance

Dose rate: 503 Gy/s
Mean beam energy: 82 keV
Continuous irradiation

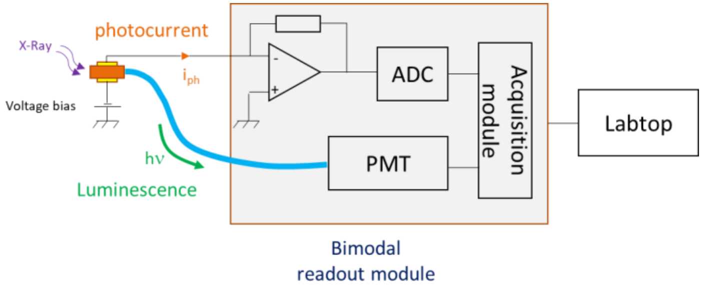

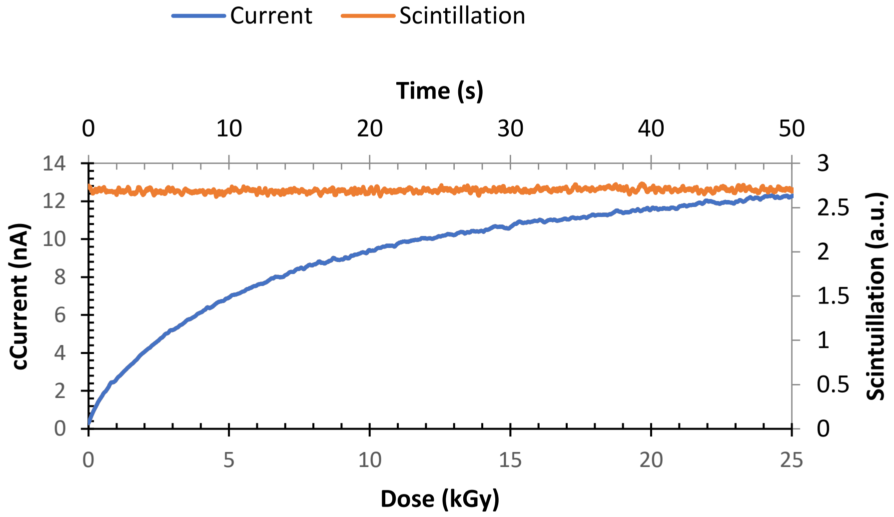

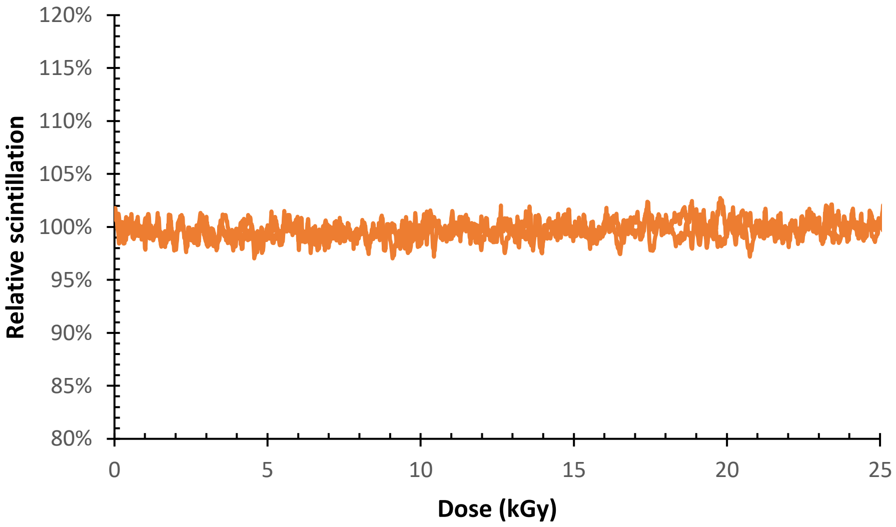

➢ PROTOTYPES EXHIBIT EXCELLENT RADIATION HARDNESS

Institut des Nanotechnologies de Lyon UMR 5270

Relative bimodal yields

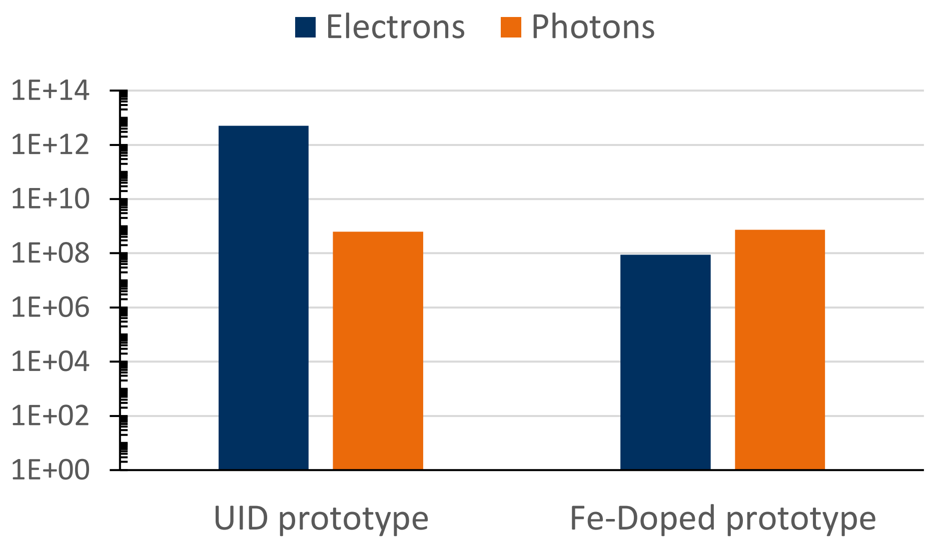

For the UID prototype, we collect 1 photon for ~10 000 electrons (~10 photons for 1 electron for Fe-doped prototype)

➢ THE PHOTOCURRENT RESPONSE CAN BE MUCH MORE SENSITIVE THAN THE SCINTILLATION ONE

Transient response

5V bias voltage

Photocurrent
Scintillation signal

Fe-doped detector

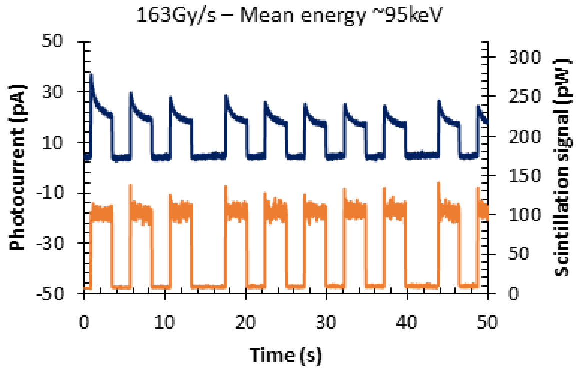

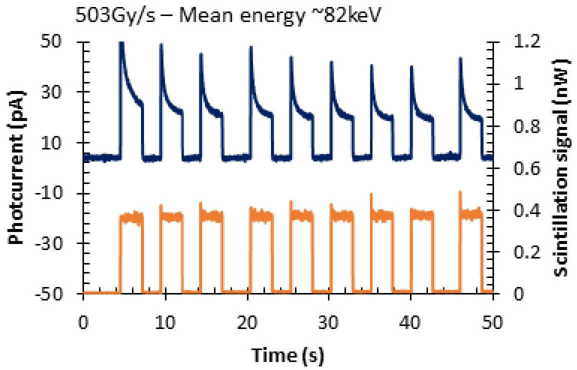

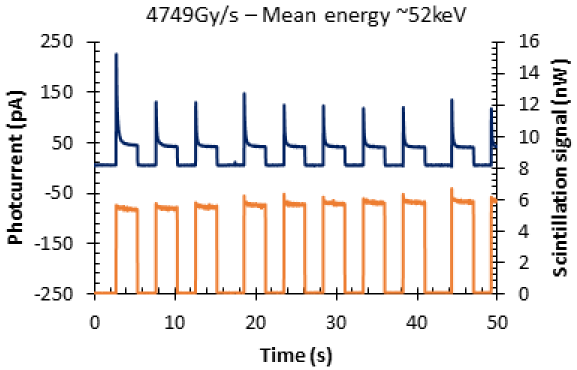

UID detector

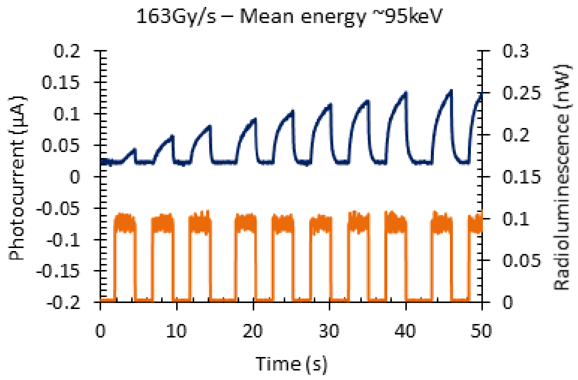

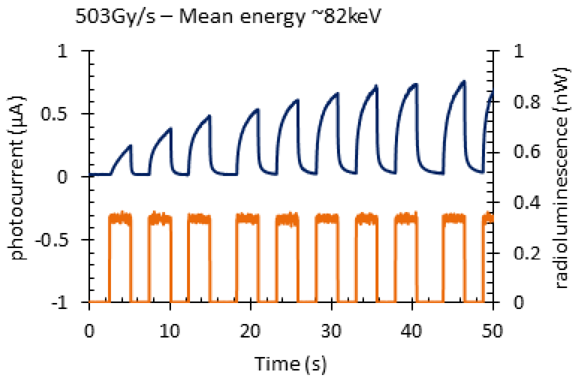

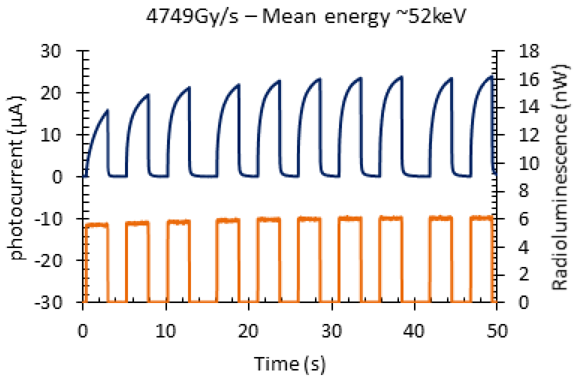

Institut des Nanotechnologies de Lyon UMR 5270

Conclusion and perspectives

BIMODAL DETECTORS

- ➢ COMBINE ADVANTAGEOUS FEATURES OF BOTH TRANSDUCTION MODES (e.g. speed & sensitivity)
- ➢ CAN IMPLEMENT A DIFFERENT SPATIAL RESOLUTION FOR EACH MODE OF TRANSDUCTION WITH A SINGLE ABSORBER MEDIUM

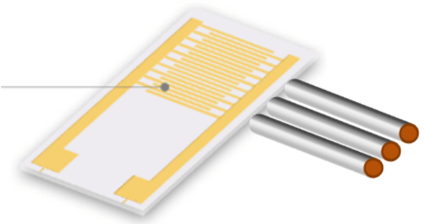

Conclusion and perspectives

BIMODAL DETECTOR PROOF-OF-CONCEPT

- COMBINE ADVANTAGEOUS FEATURES OF BOTH TRANSDUCTION MODES (e.g. speed & sensitivity)
- CAN IMPLEMENT A DIFFERENT SPATIAL RESOLUTION FOR EACH MODE OF TRANSDUCTION WITH A SINGLE ABSORBER MEDIUM

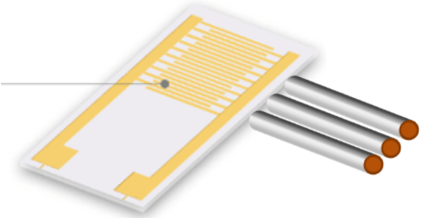

- MAY ALSO PROVE USEFUL FOR STUDYING AGING (Aging mechanisms probably affect differently the photocurrent and scintillation signal)

X-ray Beam Induced Current and Scintillation

adapted from [17]

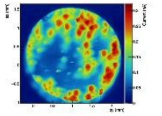

X-RAY INDUCED CURRENT MAP

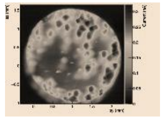

X-RAY INDUCED SCINTILLATION MAP

- MAY ALSO BE USEFUL FOR DEVELOPING A METHOD OF SELF-COMPENSATION FOR AGING (if the drifts observed in each mode do not have the same speeds)
- COULD ALSO BE IMPLEMENTED WITH SOME OTHER WBG AND UWBG SEMICONDUCTORS (e.g. GaN, ZnO, Diamond)

[17] F. Lafont, T. N. Tran Caliste, J. Baruchel, E. Capria. ESRF.

Optical Materials 169 (2026) 117697
Contents lists available at ScienceDirect
Optical Materials
journal homepage: www.elsevier.com/locate/optmat
Research Article
Photoluminescence and scintillation properties of the GaN substrate
Yuta Tominaga, Takumi Kato, Akihiro Nishikawa, Keiichiro Miyazaki,

SCIENTIFIC REPORTS
OPEN ZnO Luminescence and scintillation studied via photoexcitation, X-ray excitation, and gamma-induced positron spectroscopy

Nuclear Instruments and Methods in Physics Research A 1057 (2023) 168789
Contents lists available at ScienceDirect
Nuclear Inst. and Methods in Physics Research, A
journal homepage: www.elsevier.com/locate/nima
Basic characteristics of synthetic-diamond scintillator

Acknowledgment

THANK YOU FOR YOUR ATTENTION !

FLORIAN THEVENET, JOSUÉ ESTEVES, GUO-NENG LU, JÉRÔME DEGOUTTES, BENJAMIN FORNACCIARI, PHILIPPE NUGUES, JEAN-MARIE BLUET - INL, LYON FRANCE

JEAN-FRANCOIS ADAM, SARVENAZ KESHMIRI – STROBE UNIV. GRENOBLE ALPES, FRANCE

MICHAEL LERCH, JOHN PAUL ORTIZ BUSTILLO AND ENBANG LI – CRMP UNIV- WOLLONGONG, AUSTRALIA

CHRIS HALL AND MATHEW CAMERON – ANSTO – MELRBOURNE, AUSTRALIA

PIERRE EVERAERE , THU NHI TRAN CALISTE – ESRF – GRENOBLE, FRANCE

THE AUTHORS ACKNOWLEDGE FOR THEIR SUPPORT:

- INCA AND INSERM (PCSI / 2023 / IODA-MASTER / 23CP088)
- ANSTO (IN-KIND GRANT AS251/IMBL/23184)
- LABEX PRIMES (ANR-11-LABX-0063) LABEX PRIMES UNIVERSITÉ DE LYON
- NANOLYON PLATFORM FROM THE FRENCH NATIONAL NETWORK CNRS-RENATECH+ nanolyon RENATECH+

Institut des Nanotechnologies de Lyon UMR 5270

Back-up

Acknowledgment

Thank you for your attention !

The authors acknowledge for their support:

- InCa and Inserm (PCSI / 2023 / IODA-Master / 23CP088)
- ANSTO (in-kind grant AS251/IMBL/23184) with special thanks to Chris Hall and Mathew Cameron
- LABEX PRIMES (ANR-11-LABX-0063)
- Nanolyon platform from the French national network CNRS-RENATECH+
- Michael Lerch, John Paul Ortiz Bustillo and Enbang Li from CRMP – Univ- Wollongong

Institut des Nanotechnologies de Lyon UMR 5270

Results: Lab characterization - DUV photodetection

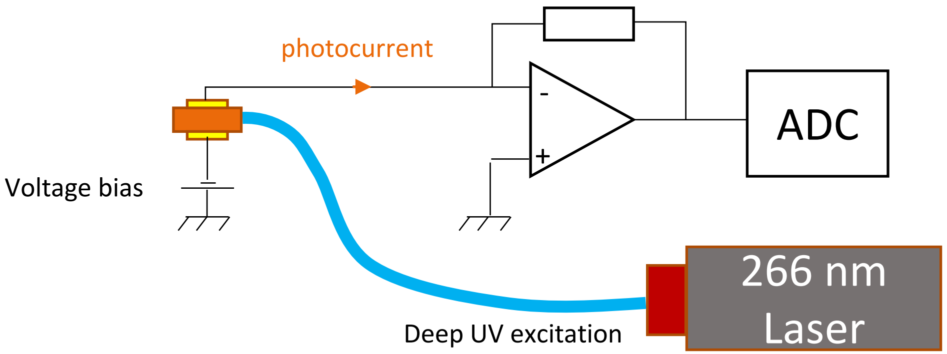

UID prototype - **No bias → ~100 pA peak-peak**

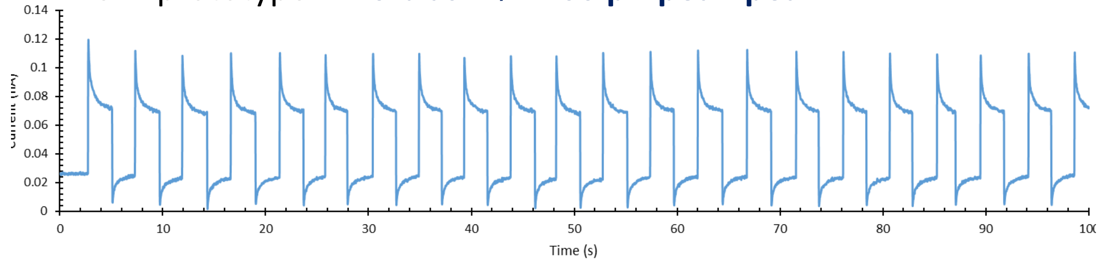

UID prototype - **6V Bias → ~300 nA peak-peak**

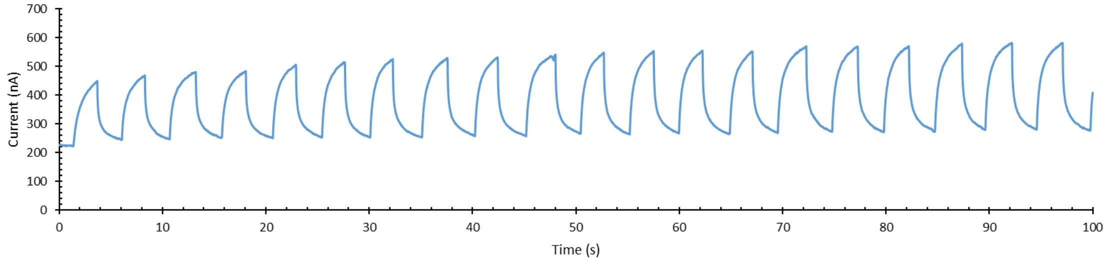

Bias voltage on the MSM structure allows:

- better charge collection efficiency
- Photoconductivity gain (but also persistent photoconductivity)

Ga2O3 MSM detector prototypes

β-Ga2O3	UID prototype	Fe-Doped prototype
Orientation	-201	010
Conductivity	n-type	Insulating ($>10^{10}\Omega.cm$)
Doping level	$\sim 2x10^{17}cm^{-3}$	-
Thickness	680µm ± 20µm	680µm ± 20µm
Surfaces	CMP/Grinding	CMP/Grinding

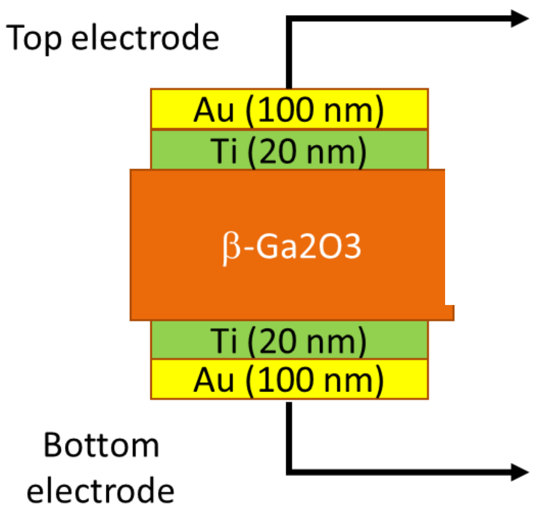

Ohmic contacts on UID β-Ga2O3

R~5Ω

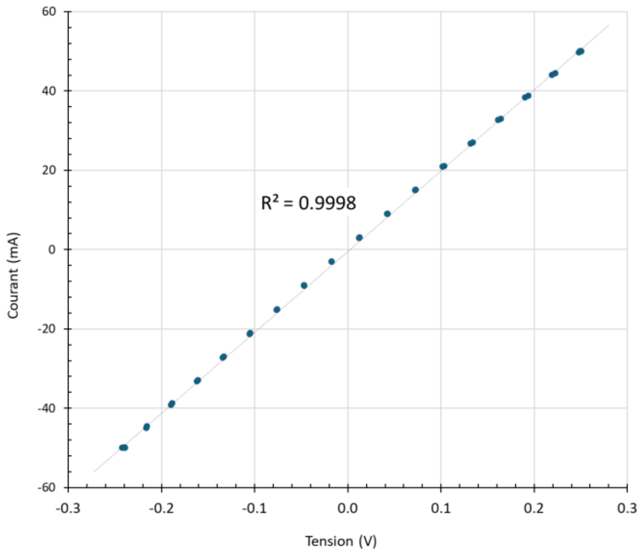

2x5 mm² Ti/Au electrodes defined by using stencils are obtained as follows:

- RIE Plasma to promote ohmic contact formation (SF6 50sccm - 30 mTorr- 200W -15 min.)
- Electron beam evaporation of Ti/Au stack
- Thermal annealed at 470°C in N2 for 10 minutes (optional)

Institut des Nanotechnologies de Lyon UMR 5270

Results: transient response

5V bias voltage

UID detector Stronger excitations give shorter transitions in the transient response

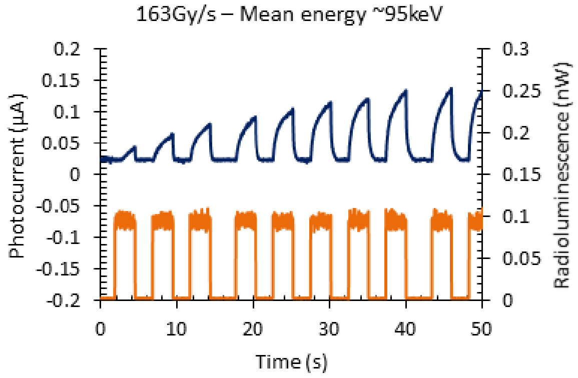

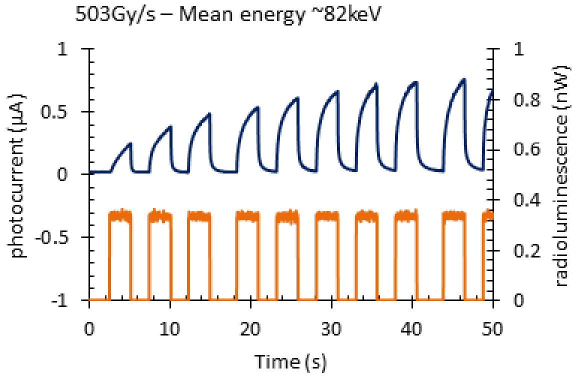

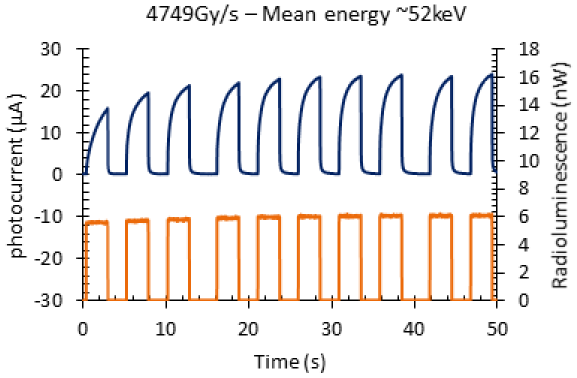

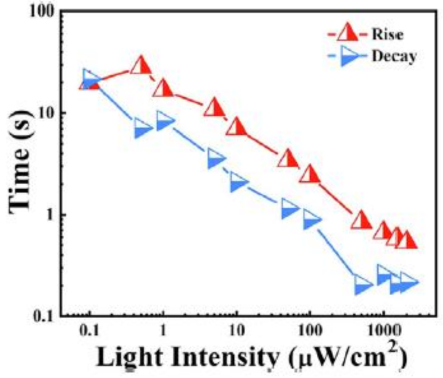

https://doi.org/10.1016/j.matdes.2022.110917

Institut des Nanotechnologies de Lyon UMR 5270

Development of Vertical Se-Ga2O3-based heterojunction detector

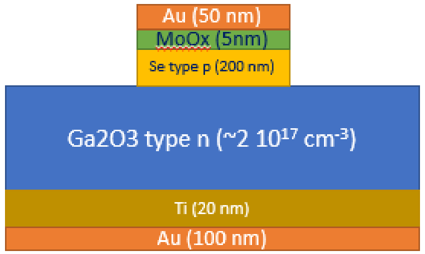

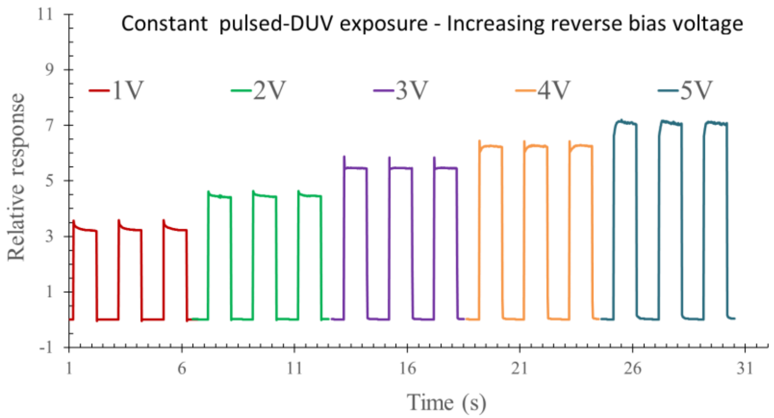

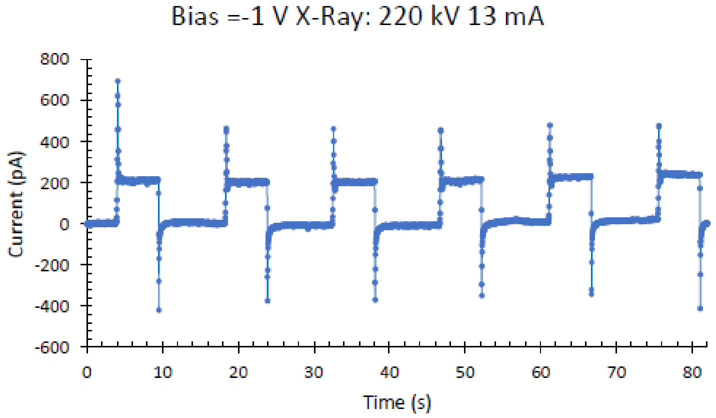

Results: ANSTO IMBL measurements

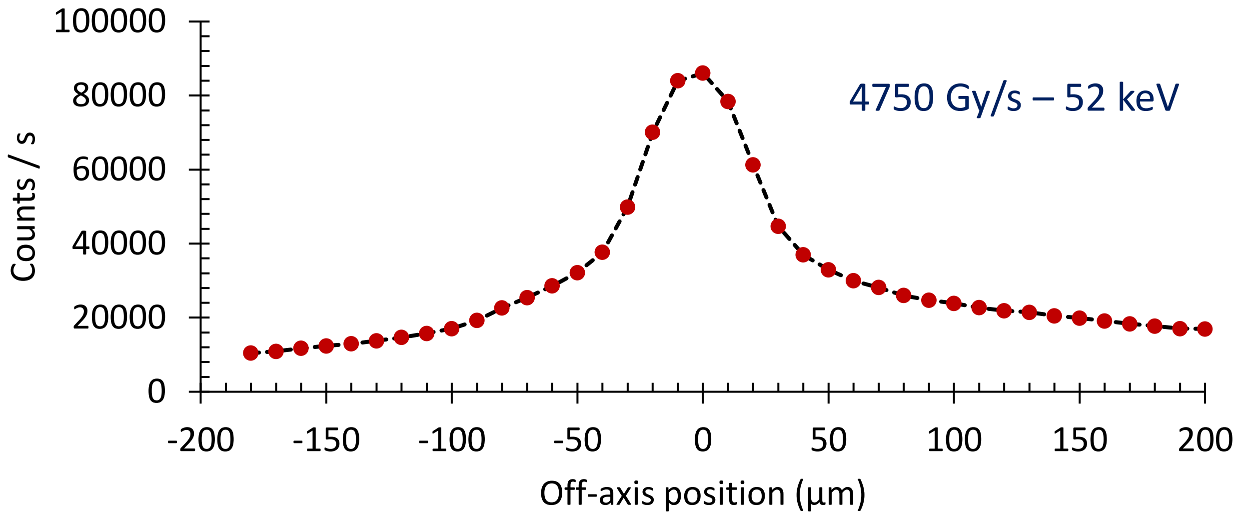

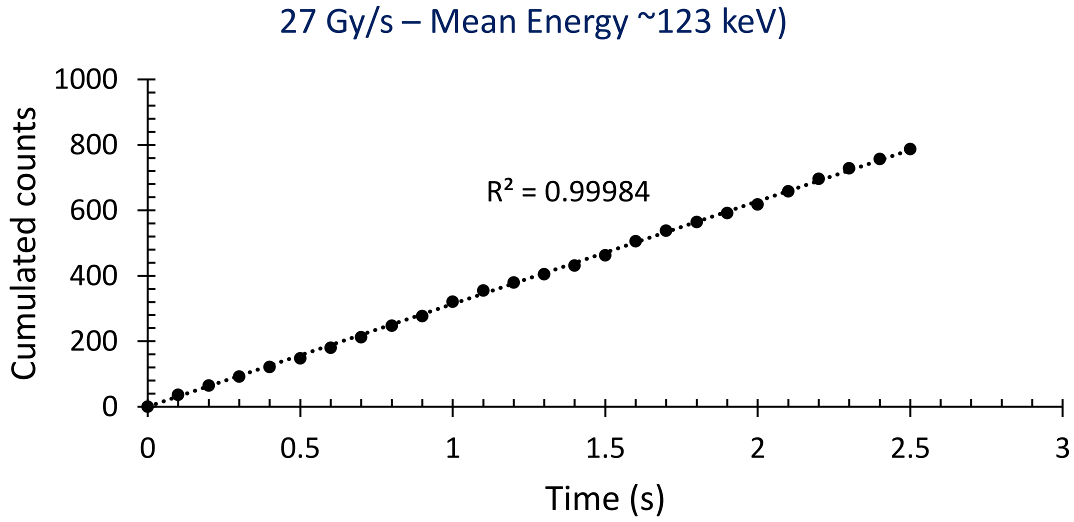

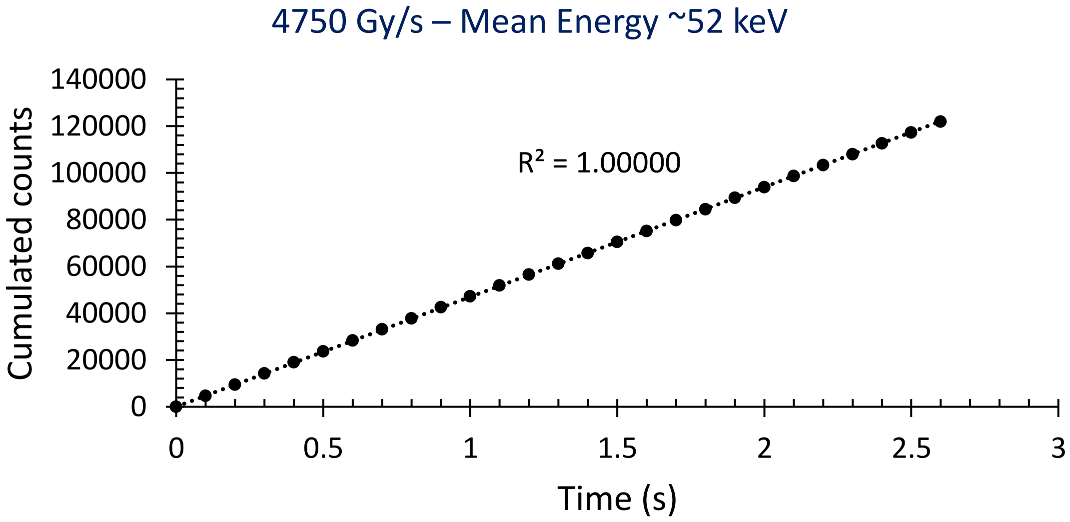

BC-408 based microstrip scintillating detector system

Yield drop between

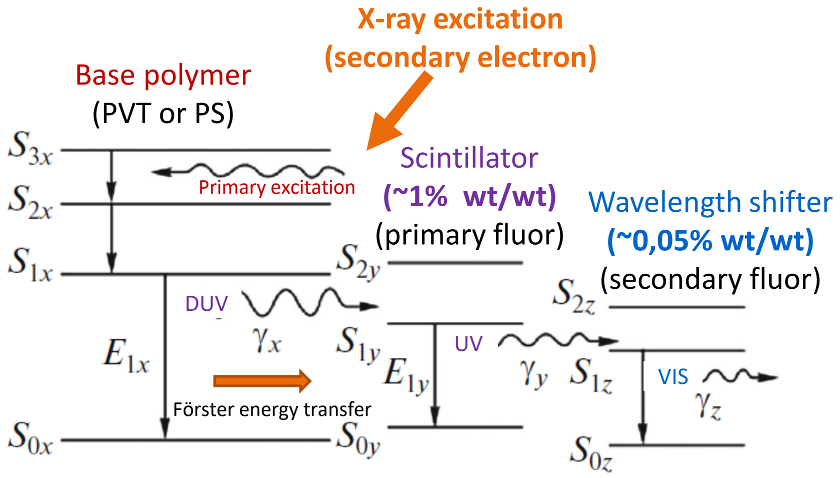

Scintillation mechanism in a three-component scintillator (Adapted from [10]*)*

- Distance between scintillator and wavelength shifter dopants is optimized in high yield plastic scintillating material (typically 150 µm [11]).
- For the 20 µm microstrips, **scintillator emission is probably absorbed in the base polymer before reaching any wavelength shifting dopant**

Institut des Nanotechnologies de Lyon UMR 5270

[10] Physics of Particles and Nuclei, 2019, Vol. 50, No. 1, pp. 42–76
[11] Leutz, Nucl. Instrum. Methods Phys. Res., 1995, A 364 pp422-448

SEM and Cathodoluminescence microstrip characterization

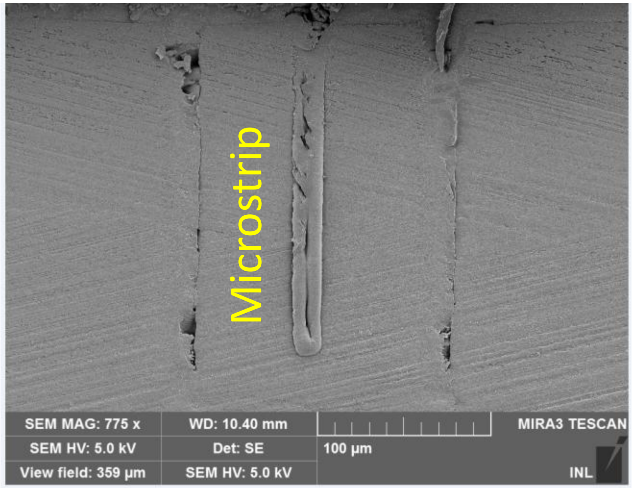

Cathodoluminescence

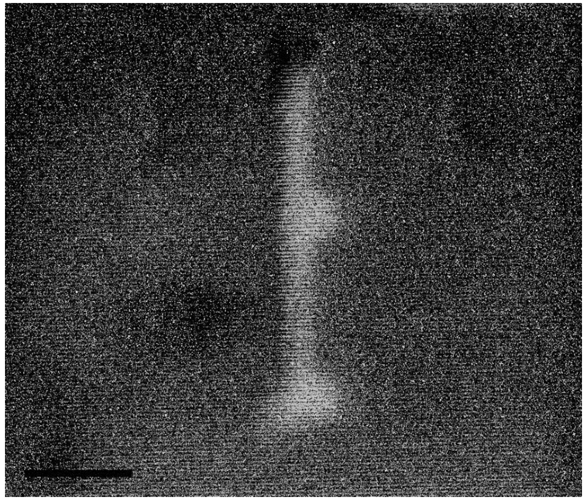

Zoom

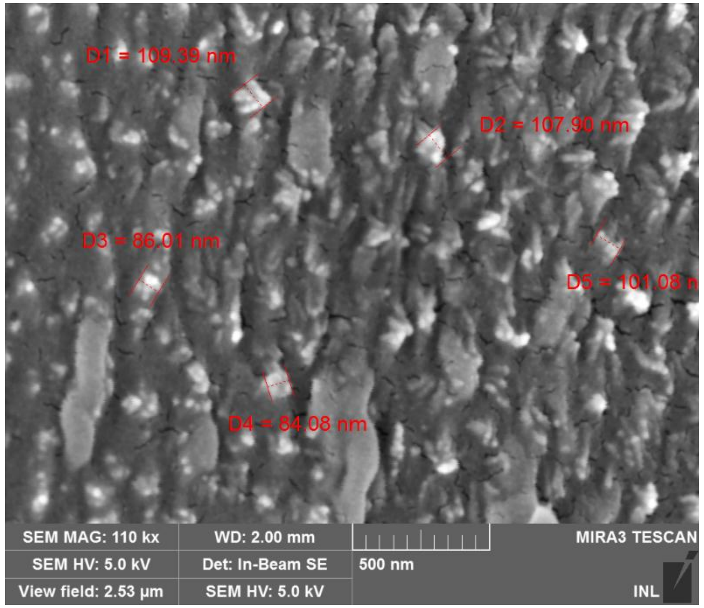

QDot size
(aggregates)
[80 nm – 110 nm]

Institut des Nanotechnologies de Lyon UMR 5270

Transient response

Fe-doped detector

5V bias voltage